

**Optimization of the Automated Spray Layer-by-Layer
Technique for Thin Film Deposition**

by

James Hart Gifford

Captain, US Army

B.S. Chemistry

United States Military Academy, West Point (2001)

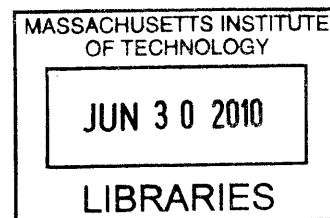
Submitted to the Department of Chemical Engineering
in partial fulfillment of the requirements for the degree of:

Master of Science

at the

Massachusetts Institute of Technology

June 2010



ARCHIVES

© 2010 Massachusetts Institute of Technology

All rights reserved

Signature of Author _____

A handwritten signature in black ink, appearing to be "J. Hart Gifford", written over a horizontal line.

Department of Chemical Engineering
May 14, 2010

Certified by _____

Paula T. Hammond
Professor of Chemical Engineering
Thesis Advisor

Signature of Author _____

William M. Deen
Professor of Chemical Engineering
Chairman, Committee for Graduate Students

Report Documentation Page		Form Approved OMB No. 0704-0188
Public reporting burden for the collection of information is estimated to average 1 hour per response, including the time for reviewing instructions, searching existing data sources, gathering and maintaining the data needed, and completing and reviewing the collection of information. Send comments regarding this burden estimate or any other aspect of this collection of information, including suggestions for reducing this burden, to Washington Headquarters Services, Directorate for Information Operations and Reports, 1215 Jefferson Davis Highway, Suite 1204, Arlington VA 22202-4302. Respondents should be aware that notwithstanding any other provision of law, no person shall be subject to a penalty for failing to comply with a collection of information if it does not display a currently valid OMB control number.		
1. REPORT DATE JUN 2010	2. REPORT TYPE	3. DATES COVERED 00-00-2010 to 00-00-2010
4. TITLE AND SUBTITLE Optimization of the Automated Spray Layer-by-Layer Technique for THin Film Deposition		5a. CONTRACT NUMBER
		5b. GRANT NUMBER
		5c. PROGRAM ELEMENT NUMBER
6. AUTHOR(S)	5d. PROJECT NUMBER	
	5e. TASK NUMBER	
	5f. WORK UNIT NUMBER	
7. PERFORMING ORGANIZATION NAME(S) AND ADDRESS(ES) Massachusetts Institute of Technology, 77 Massachusetts Avenue, Cambridge, MA, 02139		8. PERFORMING ORGANIZATION REPORT NUMBER
9. SPONSORING/MONITORING AGENCY NAME(S) AND ADDRESS(ES)		10. SPONSOR/MONITOR'S ACRONYM(S)
		11. SPONSOR/MONITOR'S REPORT NUMBER(S)
12. DISTRIBUTION/AVAILABILITY STATEMENT Approved for public release; distribution unlimited		
13. SUPPLEMENTARY NOTES		

14. ABSTRACT

The operational parameters of the automated Spray-LbL technique for thin film deposition have been investigated in order to identify their effects on film thickness and roughness. We use the automated Spray-LbL system developed at MIT by the Hammond lab to build 25 bilayer films of poly (allylamine hydrochloride) (PAH) and poly (acrylic acid) (PAA). Each of the 10 operational parameters of this system are explored individually to isolate each parameter's effect on film thickness and roughness. The parameter effects are analyzed for apparent trends to determine the parameters best suited for adjusting film thickness and roughness. The optimal parameters for thickness adjustment are polyelectrolyte solution concentration, polyelectrolyte spray time, spraying distance, air pressure and polyelectrolyte charge density. These parameters are independent of the type of species used to construct the film, and thus the trends should apply to any species used to construct thin films. The effect of each of the 10 operational parameters is examined in detail. While researching the parameter effects, polyelectrolyte interdiffusion in the films was observed. This interdiffusion is investigated using both the conventional dipped LbL and Spray-LbL deposition techniques. Interdiffusion is shown to be dependent on 3 factors, the charge density of the polyelectrolytes, the molecular weight of the polyelectrolytes, and the contact time between the polyelectrolyte solutions and the surface of the film. Interdiffusion is observed when the PAH is partially charged, the polyelectrolytes chains have a low molecular weight, and the contact time is sufficiently long enough to allow for interdiffusion. The significantly reduced contact time during the automated Spray-LbL process not only speeds up the film deposition time, but also significantly hinders the interdiffusion of PAH resulting in much thinner films than what is possible from dipping. Finally, the uniformity of the films produced using the automated Spray-LbL system is investigated. Films deposited on substrates greater than 1 in diameter area exhibit more than 20% variance in thickness. Adjustments were made to the setup of the system in an effort to expand this area of film thickness uniformity. However, it is determined that the design of this automated Spray-LbL system limits the film uniformity to an area of 1 in diameter.

15. SUBJECT TERMS

16. SECURITY CLASSIFICATION OF:

a. REPORT

unclassified

b. ABSTRACT

unclassified

c. THIS PAGE

unclassified17. LIMITATION OF
ABSTRACT**Same as
Report (SAR)**18. NUMBER
OF PAGES**88**19a. NAME OF
RESPONSIBLE PERSON

Optimization of the Automated Spray Layer-by-Layer Technique for Thin Film Deposition

by

James Hart Gifford

Submitted to the Department of Chemical Engineering
on May 14, 2010, in partial fulfillment of the
requirements for the degree of
Master of Science

Abstract

The operational parameters of the automated Spray-LbL technique for thin film deposition have been investigated in order to identify their effects on film thickness and roughness. We use the automated Spray-LbL system developed at MIT by the Hammond lab to build 25 bilayer films of poly (ally amine hydrochloride) (PAH) and poly (acrylic acid) (PAA). Each of the 10 operational parameters of this system are explored individually to isolate each parameter's effect on film thickness and roughness. The parameter effects are analyzed for apparent trends to determine the parameters best suited for adjusting film thickness and roughness. The optimal parameters for thickness adjustment are polyelectrolyte solution concentration, polyelectrolyte spray time, spraying distance, air pressure and polyelectrolyte charge density. These parameters are independent of the type of species used to construct the film, and thus the trends should apply to any species used to construct thin films. The effect of each of the 10 operational parameters is examined in detail.

While researching the parameter effects, polyelectrolyte interdiffusion in the films was observed. This interdiffusion is investigated using both the conventional dipped LbL and Spray-LbL deposition techniques. Interdiffusion is shown to be dependent on 3 factors, the charge density of the polyelectrolytes, the molecular weight of the polyelectrolytes, and the contact time between the polyelectrolyte solutions and the surface of the film. Interdiffusion is observed when the PAH is partially charged, the polyelectrolytes chains have a low molecular weight, and the contact time is sufficiently long enough to allow for interdiffusion. The significantly reduced contact time during the automated Spray-LbL process not only speeds up the film deposition time, but also significantly hinders the interdiffusion of PAH resulting in much thinner films than what is possible from dipping.

Finally, the uniformity of the films produced using the automated Spray-LbL system is investigated. Films deposited on substrates greater than 1 in diameter area exhibit more than 20% variance in thickness. Adjustments were made to the setup of the system in an effort to expand this area of film thickness uniformity. However, it is determined that the design of this automated Spray-LbL system limits the film uniformity to an area of 1 in diameter.

Thesis Supervisor: Paula T. Hammond

Title: Bayer Chair Professor of Chemical Engineering and Executive Officer

To my family, Natalie, Cole, Alli, Avery, and Cooper.

You make life worth living and I love you all.

Acknowledgements

I would like to acknowledge many people for their assistance in my completion of this thesis:

First, and foremost I would like to thank my wife, Natalie. While I was busy living the life of a grad school student, she was extremely busy running our household of five, homeschooling our son and volunteering. She amazes me every single day. I know that her accomplishments during my time at MIT will not be published or rewarded like mine, but I am positive that without her unending devotion to our family I would not be where I am today. I will never be able to thank her enough for all that she does for me or our children.

I would also like to thank my children, Cole, Alli, and Avery, for their ability to remind me that there is more to life than multilayered thin films. I am so glad that being in graduate school actually allowed me so much family time with them. The late nights and early mornings I spent doing work were worth it, because they allowed me to come home early most days to spend time with them. The afternoons that we played “fireball” and our camp outs are as important to me as this thesis.

I would like to thank my advisor, Professor Paula Hammond. I feel extremely fortunate for the opportunity to have worked for such a distinguished leader in the field of Layer-by-Layer. Your support, advice and understanding with my family situation truly helped me to excel during my time at MIT.

There are a few members of the Hammond research group that I would like to thank as well:

Kevin Krogman. Thank you for pointing me in the right direction and your unending support. I do not think there has been a two week period in the last year and a half that I haven’t asked you for some advice or help. I truly appreciate your mentorship and support.

Kittipong Saetia. Our discussions about this work were vital in helping my understanding of layer by layer process as well as the interdiffusion phenomenon. I wish you the best of luck as you continue your research.

Ray Samuel and Anita Shukla. Thank you for your help with dipping. Regardless of my aversion to the dipping process, you were instrumental in helping me obtain the dipped samples presented in this thesis.

Finally I would like to thank the US Army for the opportunity to pretend to be a normal civilian for two years.

This work made use of the Shared Experimental Facilities at MIT’s Center for Materials Science and Engineering, supported in part by the MRSEC program of the National Science Foundation under award number DMR 02-13282. It was financially supported by the U.S. Army through the Institute for Soldier Nanotechnologies, under contract DAAD-19-02-D-0002 with the U.S. Army Research Office. The content does not necessarily reflect the position of the government, and no official endorsement should be inferred.

Table of Contents

ABSTRACT	2
DEDICATION	3
ACKNOWLEDGEMENTS	4
TABLE OF CONTENTS	5
LIST OF FIGURES	7
LIST OF TABLES	10
INTRODUCTION	11
1. AUTOMATED SPRAY-LBL PARAMETER OPTIMIZATION.....	14
ABSTRACT	14
1.1 INTRODUCTION.....	14
1.2 EXPERIMENTAL.....	16
1.2.1 Materials.....	16
1.2.2 Deposition.....	16
1.2.3 Analysis.....	18
1.3 RESULTS AND DISCUSSION.....	19
1.3.1 OPTIMAL PARAMETERS FOR THIN FILM FINE-TUNING.....	19
1.3.1.1 POLYELECTROLYTE CONCENTRATION.....	20
1.3.1.2 POLYELECTROLYTE SPRAY TIME.....	24
1.3.1.3 SPRAY DISTANCE.....	26
1.3.1.4 AIR PRESSURE.....	31
1.3.1.5 POLYELECTROLYTE CHARGE DENSITY.....	34
1.3.2 THE EFFECTS OF THE OTHER PARAMETERS.....	37
1.3.2.1 POLYELECTROLYTE MOLECULAR WEIGHT.....	37
1.3.2.2 NUMBER OF AIR BRUSH TURNS.....	40
1.3.2.3 RINSE TIME.....	43
1.3.2.4 ADDITIONAL SOLVENTS.....	46
1.3.2.5 NUMBER OF BILAYERS.....	49
1.4 CONCLUSION.....	51
2. LIMITING POLYELECTROLYTE INTERDIFFUSION	51
ABSTRACT.....	51
2.1 INTRODUCTION.....	52
2.2 EXPERIMENTAL.....	53
2.2.1 MATERIALS.....	54
2.2.2 DEPOSITION.....	55
2.2.3 ANALYSIS.....	55

2.3 RESULTS AND DISCUSSION.....	56
2.4 CONCLUSION.....	67
3. FILM UNIFORMITY	68
ABSTRACT.....	68
3.1 INTRODUCTION.....	68
3.2 EXPERIMENTAL.....	69
3.2.1 MATERIALS.....	69
3.2.2 DEPOSITION.....	70
3.2.3 ANALYSIS.....	70
3.3 RESULTS AND DISCUSSION.....	71
3.4 CONCLUSION	79
CONCLUSION AND FUTURE RECOMMENDATIONS	79
REFERENCES	82
APPENDIX	84

List of Figures

FIGURE 1. LOCATIONS OF THICKNESS AND ROUGHNESS MEASUREMENTS.....	19
FIGURE 2. CORRELATION OF FILM THICKNESS TO PAA CONCENTRATION.....	20
FIGURE 3. CORRELATION OF FILM THICKNESS TO PAA CONCENTRATION BY DIPPING	22
FIGURE 4. CORRELATION OF FILM ROUGHNESS TO PAA CONCENTRATIONS.....	23
FIGURE 5. CORRELATION OF FILM THICKNESS TO PAA SPRAY TIME.....	25
FIGURE 6. CORRELATION OF FILM ROUGHNESS TO PAA SPRAY TIME.....	26
FIGURE 7. CORRELATION OF FILM THICKNESS TO SPRAYING DISTANCE.....	27
FIGURE 8. WATER FILM FORMED UPON DROPLET IMPACT WITH THE SURFACE.....	29
FIGURE 9. CORRELATION OF FILM ROUGHNESS TO SPRAY DISTANCE.....	30
FIGURE 10. CORRELATION OF FILM THICKNESS TO AIR PRESSURE.....	32
FIGURE 11. CORRELATION OF FILM ROUGHNESS TO AIR PRESSURE	33
FIGURE 12. CORRELATION OF FILM THICKNESS TO PAA PH.....	35
FIGURE 13. CORRELATION OF FILM ROUGHNESS TO PAA PH	36
FIGURE 14. CORRELATION OF FILM THICKNESS TO PAA MOLECULAR WEIGHT.....	38
FIGURE 15. CORRELATION OF FILM ROUGHNESS TO PAA MOLECULAR WEIGHT.....	39
FIGURE 16. CORRELATION OF FILM THICKNESS TO PAA AIRBRUSH TURNS.....	42

FIGURE 17. CORRELATION OF FILM ROUGHNESS TO PAA AIRBRUSH TURNS.....	43
FIGURE 18. CORRELATION OF FILM THICKNESS TO RINSE TIME.....	45
FIGURE 19. CORRELATION OF FILM ROUGHNESS TO RINSE TIME.....	46
FIGURE 20. CORRELATION OF FILM THICKNESS TO THE ADDITIONAL SOLVENT ADDED TO THE PAA SOLUTION.....	47
FIGURE 21. CORRELATION OF FILM ROUGHNESS TO THE ADDITIONAL SOLVENT ADDED TO THE PAA SOLUTION.....	48
FIGURE 22. CORRELATION OF FILM THICKNESS TO THE NUMBER OF BILAYERS.....	49
FIGURE 23. CORRELATION OF FILM ROUGHNESS TO THE NUMBER OF BILAYERS.....	50
FIGURE 24. GROWTH CURVES FOR SPRAYED AND DIPPED (PAH/PAA) ₂₅ FILMS.....	58
FIGURE 25. CORRELATION OF BILAYER THICKNESS TO THE NUMBER OF BILAYERS BOTH DIPPED AND SPRAYED.....	63
FIGURE 26. GROWTH RATE OF TOP PAA LAYER.....	65
FIGURE 27. LOCATIONS OF THICKNESS MEASUREMENTS TAKEN FOR FILM UNIFORMITY.....	70
FIGURE 28. 3-D PLOT OF FILM THICKNESS OF A STANDARD (PAH/PAA) ₂₅ FILM.....	72
FIGURE 29. PARALLEL 3-D VIEW OF THE FILM THICKNESS OF A STANDARD (PAH/PAA) ₂₅ FILM.....	73

FIGURE 30. PARALLEL 3-D VIEW OF THE FILM THICKNESS OF A (PAH/PAA)₂₅ FILM

WITH SPRAYING DISTANCE OF 10 INCHES.....74

FIGURE 31. AIM POINTS USED TO EXAMINE FILM UNIFORMITY..... 75

FIGURE 32. PARALLEL 3-D VIEW OF THE FILM THICKNESS OF A (PAH/PAA)₂₅ FILM

WITH OFFSET AIM POINTS.....76

FIGURE 33. PARALLEL 3-D VIEW OF THE FILM THICKNESS OF A (PAH/PAA)₂₅ FILM

WITH AIM POINTS AT THE EDGES OF THE SUBSTRATE.....77

FIGURE 34. PERCENT REFLECTANCE DATA FOR A ((PADC/ SiO₂)₂₅ FILM

DEPOSITED USING A LARGER SPRAY-LBL SYSTEM.....78

List of Tables

TABLE 1. LIST OF THE 10 OPERATIONAL PARAMETERS OF THE AUTOMATED

SPRAY-LBL SYSTEM AND THEIR STANDARD VALUES FOR THIS RESEACH.....17

TABLE 2. IMPACT VELOCITY OF THE PAA SOLUTION DROPLETS AT THE ADJUSTED

SPRAYING DISTANCES.....28

TABLE 3. EXIT AND IMPACT VELOCITY OF THE PAA SOLUTION DROPLETS AT THE

ADJUSTED AIR PRESSURES.....31

TABLE 4. FLOW RATES OF THE PAA SOLUTION AT EACH VALUE OF AIRBRUSH TURNS.....41

TABLE 5. AVERAGE BILAYER THICKNESS OF (PAH/PAA)₂₅ FILMS MADE USING DIFFERENT

COMBINATIONS OF PAA MOLECULAR WEIGHTS AND PAH SOLUTION PH VALUES.....57

TABLE 6. AVERAGE BILAYER THICKNESS OF (PAH/PAA)₂₅ USING BOTH DEPOSITION TECHNIQUES

AT 20 MMOL CONCENTRATION.....61

Introduction

The layer-by-layer (LbL) thin film deposition process is an established method to produce highly tunable thin films on the nanometer scale.¹ This process involves sequentially exposing a substrate to oppositely functionalized species in order to construct a multilayered film on the substrate. Early work on multilayered films began in the 1960s and 1970s with oppositely charged metal oxide particles and glass substrates.^{2, 3} In the late 1980s Decher and co-workers first deposited polyelectrolyte films onto glass substrates, laying the groundwork for LbL as we know it today. Polyelectrolytes are extremely useful in multilayered thin films because they are long polymer chains with varying amounts of charge along the chain. It is this multi-charged nature of the polymer chains that allows for the charge reversal of the film surface and the subsequent adsorption of the next layer. Without the charge reversal, the like charged species would continue to adsorb to the surface, and the oppositely charged species would not adsorb to the surface; producing a thick monolayered film. The charge reversal is the key to multilayered thin films, as it is this self-limiting process that keeps these films thin and multilayered. Today, films are still assembled using the electrostatic interactions between strong^{1, 2} or weak polyelectrolytes³; however, the LbL process has been expanded to incorporate films using biomolecules^{4, 5}, carbon nanotubes⁶, colloidal nanomaterials^{7, 8} and through hydrogen bonding mechanisms⁹⁻¹². As the species utilized in LbL deposition has expanded, so have the applications of LbL deposition. LbL thin films now have a variety of applications, including drug delivery¹³, antireflective coatings¹⁴, batteries¹⁵, electrochromic devices¹⁶, and chemical warfare protection.⁸

Typically this process is conducted by dipping a substrate with a surface charge into a weak solution of an oppositely charged polyelectrolyte and allowing the polyelectrolyte chains in solution to diffuse to the substrate surface and form electrostatic bonds with the charged surface. The driving force for this process is the concentration gradient and electrostatic potential gradient between the solution and the substrate or film surface. As the oppositely charged polyelectrolyte chains adsorb onto the

surface, the surface experiences a charge reversal. The substrate is then rinsed in water to remove any loosely bound polyelectrolyte from the surface and the substrate is then dipped into the oppositely charged polyelectrolyte solution and a subsequent rinse to complete the construction of one bilayer. The LbL adsorption process is thus cycled through these steps until the desired number of bilayers is achieved; the assembly time of a typical bilayer is on the order of 30 minutes.

In an effort to reduce this bilayer assembly time, a variation of the LbL process has been developed, automated Spray-LbL, which consists of spraying the polyelectrolyte and rinse solutions directly onto a stationary vertical substrate.^{2, 7, 17} The convection of the spray droplets to the substrate surface created by the high pressure gas is the main driving force for Spray-LbL. As the droplets impact the surface, the polyelectrolyte chains must diffuse across a micron scale thin water film resulting from the drop impingement on the substrate, and onto the charged surface. The Spray-LbL method exposes the substrate to this atomized spray of polyelectrolyte solution for a short period of time, typically 3-10 seconds. Then after a few seconds to allow the excess solution to drain off, the substrate is sprayed with rinse water to remove any loosely bound polyelectrolytes. The surface experiences a charge reversal as the polyelectrolyte chains adsorb onto the surface from the droplets. Next the oppositely charged polyelectrolyte is sprayed onto the surface and allowed to drain. The substrate is then rinsed and the bilayer is completed. Normal bilayer assembly times for Spray-LbL range from 30-60 seconds, an order of magnitude decrease in film assembly time.

It has been demonstrated that the Spray-LbL technique produces thin films that are similar to films deposited using the traditional dipped process, except that the films are produced much faster.^{7, 17} A 25 bilayer dipped film typically takes more than 11 hours to deposit, whereas the same film takes less than 20 minutes to deposit using Spray-LbL. This significantly reduced process time is the main advantage of Spray-LbL over dipped LbL. Another appealing aspect of Spray-LbL is the reduction in

waste for a sprayed film. To effectively deposit a thin film onto a substrate using dipped LbL requires solution baths that are large enough to allow for submersion of the substrate and a large amount of solution to provide enough of the necessary species molecules to adsorb to the surface. Also, due to the sequential dipping process some contamination of solutions from the oppositely charged species is unavoidable, making reuse of the solutions not possible. On the other hand, Spray-LbL requires only enough solution to spray each layer for a few seconds. Any unsprayed solution is completely reusable, since there is no cross contamination in the spray process. The other significant advantage of Spray-LbL over dipped LbL is its scalability. As previously discussed, the dipped LbL process requires solution baths larger than the substrate itself. It would be extremely difficult to deposit a film onto a substrate larger than a few inches by dip LbL, because the size of the solution baths as well as the ability to move and dip the substrate into these baths. However, with Spray-LbL coating a larger substrate would be possible with only the addition of more nozzles to the spraying assembly. These advantages of automated Spray-LbL make it a desirable process for depositing multilayered thin films; however, automated Spray-LbL is still relatively new with little understanding of the effect of the different parameters on the deposition process.

In the work presented here the effect on film thickness and roughness of the 10 operational parameters of the Spray-LbL system previously developed by the Hammond lab⁷ will be investigated. Once each parameter's effect is quantified and trends are determined, the parameters best suited for adjusting film thickness and/or film roughness will be identified. During this research into the parameter effects, two other discoveries were made and are discussed here. First, the interdiffusion phenomenon known to occur in partially charged polyelectrolyte films is notably less prevalent in sprayed films than in dipped films. This is expected based on the reduced spraying contact time, but has not been previously demonstrated. Second, the uniformity of the films produced by this Spray-LbL system is investigated to determine the limit of the substrate size that can be coated using this system.

1. Automated Spray-LbL Parameter Optimization

Abstract

The operational parameters of the automated Spray-LbL technique in thin film deposition have been investigated for their effects on film thickness and roughness. We use the fully automated Spray-LbL system developed at MIT by the Hammond lab to build 25 bilayer films of Poly (ally amine hydrochloride) (PAH) and poly (acrylic acid) (PAA). Each of the 10 operational parameters of this system are investigated individually to isolate each parameter's effect on film thickness and roughness. The parameter effects are then analyzed for trends to determine the parameters most suited for adjusting film thickness and/ or roughness. The parameters for film thickness adjustment are polyelectrolyte solution concentration, polyelectrolyte contact time, spraying distance, air pressure and polyelectrolyte charge density. These parameters are independent of the type of species used to construct the film, and thus the trends should apply to any polymer species used to construct thin films. In examining film roughness, no optimal parameters were found. The effect of each of the 10 operational parameters is examined in detail.

1.1 Introduction

Since the late 1990s, the layer by layer technique for the deposition of polyelectrolytes to produce thin films of operational thickness at the nanometer length scale¹ has found widespread use in a variety of applications. By alternately exposing a charged substrate to oppositely charged polyelectrolytes, layers of the polyelectrolytes build up through electrostatic binding. This process is typically carried out by alternately submerging the substrate into polyelectrolyte solutions. As the charged surface is submerged in the solution, the polyelectrolyte chains near the surface adsorb onto

the surface. This creates a concentration gradient between the bulk solution and the substrate surface, driving the polyelectrolyte molecules in the bulk solution to diffuse to the substrate. This diffusion is not a rapid process and requires several minutes to be completed. This reliance on the diffusion time scales indicates that films of more than a few bilayers will require hours to deposit.

In an effort to reduce the deposition time, a new LbL technique known as automated Spray-LbL was developed. This new process consists of spraying the polyelectrolytes directly onto a stationary vertical substrate.^{2, 7, 17} By spraying small droplets of the polyelectrolyte solution uniformly over the entire substrate at once, the diffusion length of the polyelectrolyte chains from the bulk solution to the substrate surface is significantly reduced. We are able to directly contact the surface with micron scale polyelectrolyte solution droplets, so the polyelectrolyte chains inside the droplets only have to diffuse a few microns as opposed to the millimeters they would have to diffuse in the bulk solution. This significantly reduces the contact time necessary to deposit films, making film deposition on the order of minutes instead of hours. Spray-LbL systems have been developed by numerous people ranging from simple hand-operated spray bottles² and air-pumped spray-paint cans^{17, 18} to fully automated systems using high pressure gas.^{7, 19} This work uses the automated spray system previously developed by the Hammond lab at MIT,⁷ to examine the impact of process parameters that are readily controlled with full automation and independently manipulated.

Since the first time polyelectrolytes were sprayed onto a substrate to produce a film, research has focused on comparing those films to films deposited using the dipping technique because the dipping technique is well known and understood. However, automated Spray-LbL offers speed and more controllable parameters than the dipping process, and potentially more control over thin film deposition. The purpose of the research in this chapter was to determine which of the 10 operational parameters of this system are best suited for controlling film thickness and/or roughness. Each of these

operational parameters was adjusted individually to isolate its effect on the films. By analyzing trends, it was possible to identify which trends affect the film thickness and/or roughness in a operational manner and which parameters do not.

1.2 Experimental

1.2.1 Materials

Poly (acrylic acid, sodium salt) (PAA) with molecular weight of 15,000 g/mol (35% aqueous solution) and molecular weight of 1,250,000 (powder) was purchased from Sigma Aldrich. Poly(acrylic acid) (PAA) molecular weight of 345,000 g/mol (25% aqueous solution) and Poly(ally amine hydrochloride) (PAH) molecular weight of 55 000 (powder) was purchased from Polysciences. Polymer solutions were prepared using Milli-Q water with a standard concentration of 20 mmol with respect to the repeat unit, except when examining concentration effects. PAH solutions were prepared at a pH of 9.0 ($pK_a \sim 8.8^{20}$) and PAA solutions were prepared at a pH of 6.5 ($pK_a \sim 6.5^{20}$), except when examining pH effects. All solution pH adjustment was performed using HCl and NaOH, no additional salt was added to the polyelectrolyte or rinse solutions. Spray-LbL films were deposited on 3-inch coin roll silicon wafers (Silicon Quest International), and dipped LbL films were deposited on similar wafers that had been cut into 1cm x 3 cm pieces. All silicon was cleaned with ethanol and Milli-Q water to clean and hydroxylate the surface prior to deposition.

1.2.2 Deposition

Sprayed films were constructed using the automated Spray-LbL system.⁷ All spray solutions were delivered by ultra high purity nitrogen gas (AirGas) regulated to 25psi, except when examining air

pressure effects. The PAH solution was sprayed for 4 s and allowed to drain for 5 s before spraying the rinse solution for 10 s, except when examining spraying time effects. After 5 s for rinse drainage, the PAA solution was sprayed and rinsed similarly. This cycle was then repeated for the desired number of bilayers, with an additional 6 s pause between bilayers. Using this setup a 25 bilayer film required approximately 20.4 min for complete deposition.

10 parameters of the Spray-LBL system have been identified as operational and were adjusted individually during deposition. A standard value for each parameter was chosen based on typical film deposition of this system. The adjustable parameters and their standard values are listed in Table 1. To isolate the effects of each parameter, the other nine parameters were kept constant at their standard value. This allowed for easy trend isolation and identification for each of the 10 operational parameters.

Table 1. List of the 10 operational parameters of the automated Spray-LbL system and their standard values for this research.

Controllable Parameters	Species	Standard Value	Units
Molecular Weight	PAH	65 000	Da
	PAA	15 000	Da
Solution Concentration	PAH	20 *	mmol
	PAA	20	mmol
Air Pressure		25	psi
Solution pH	PAH	9.0 *	
	PAA	6.5	
Solvent		Water Only	
Spray Distance		7.5	in.
Airbrush Needle Turns	PAH	5 *	
	PAA	5	
Spray Time	PAH	4 *	s
	PAA	4	s
	Rinse	10	s
Number of Bilayers		25	

* Held constant for all films.

Dipped films used for comparison were constructed using a Carl Zeiss HMS DS-50 slide stainer. Identical polyelectrolyte solutions were used for dipping. The cleaned substrates were first submerged in the PAH solution for 10 min followed by two, 1 min rinse steps in Milli-Q water at its default pH. The substrate was then submerged in the PAA solution and rinsed by an additional two, 1 min rinse steps in Milli-Q water. This cycle was then repeated for the required number of bilayers. After the final rinse step, the substrate was removed from the final rinse bath and dried thoroughly. Using this setup a 25 bilayer film required approximately 12.5 h for complete deposition.

1.2.3 Analysis

Film thickness was measured using a Tencor P16 profilometer to drag a stylus across a scored film to determine the step height. A stylus tip force of 0.5 mg was used to avoid film penetration. Eight measurements from different locations on the film were taken to ensure a good average value of film thickness, Figure 1. Thickness measurements were verified using a Woolam XLS-100 spectroscopic ellipsometer. Roughness values were also measured using the Tencor P-16 profilometer in a similar manner. Four roughness measurements were taken from different locations on the film, Figure 1. The roughness values presented are the root mean square (RMS) values determined by the profilometer. Films were dried in a nitrogen stream prior to measurement to remove any dust or other particles from the film surface.

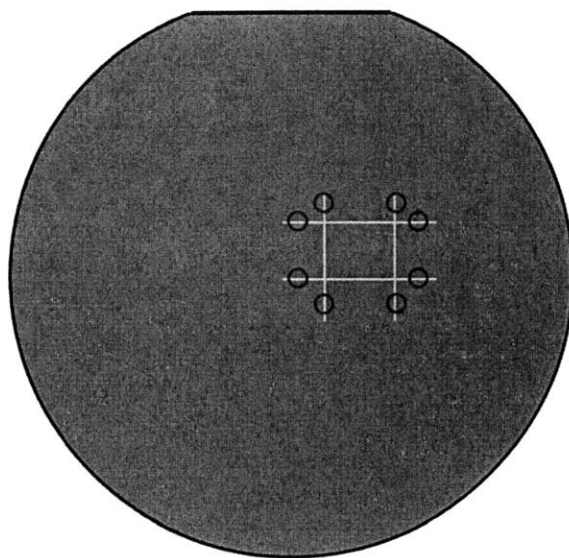


Figure 1. Locations of thickness and roughness measurements. The yellow number sign was scratched into the film using a razor blade, and thickness measurements were taken where the eight red circles are located. One roughness measurements were taken in the location of each of the four blue lines. Each roughness measurement was taken over length of 900 nm.

1.3 Results and Discussion

1.3.1 Optimal Parameters for Thin Film Fine-tuning

Each of the 10 operational parameters of the automated Spray-LbL system were adjusted individually and systematically to determine the best parameters to control and adjust the film thickness and roughness. Five of the 10 operational parameters exhibited clear trends in film thickness. Each of these parameters can be adjusted to produce either thicker or thinner films with some level of accuracy. These five parameters are polyelectrolyte concentration, polyelectrolyte spray time, the distance between the spray nozzles and the substrate, the air pressure and the polyelectrolyte charge density.

Instead of looking for clear trends in film roughness, this work was focused on finding the values of the parameters that resulted in the smoothest possible films.

1.3.1.1 Polyelectrolyte Concentration.

Concentration is occasionally used to adjust the film thickness in dipped LbL.²¹ For this work, the concentration of the PAA solution was the only parameter adjusted from the standard sample (Table 1) and the concentration of the PAH solution was held at 20 mmol. PAA concentration was adjusted from 10 mmol to a concentration of 200 mmol, much higher than typical LbL concentrations. The resulting thickness trend is shown in Figure 2.

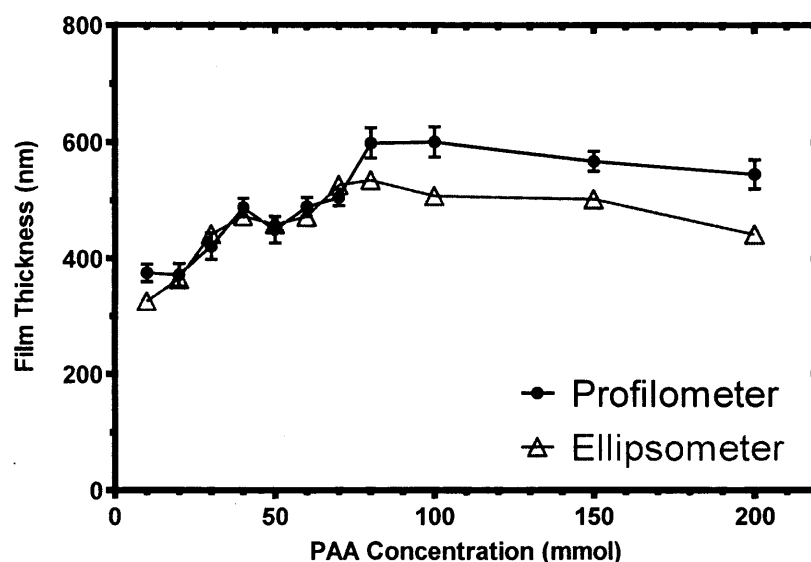


Figure 2. Correlation of film thickness to PAA concentration.

From (PAH/PAA)₂₅ films deposited by automated Spray-LbL. Film show an increase in thickness as the PAA concentration increases up to a maximum possible thickness at 80 mmol concentration.

As the polyelectrolyte concentration increases, the overall film thickness also increases. Increasing the polyelectrolyte concentration, will increase the number of polyelectrolyte molecules in each sprayed droplet. Having more polyelectrolyte molecules in each droplet will require less time for a specific number of polyelectrolyte chains to adsorb to the surface once the droplets impact the surface and spread into a liquid film on the surface. Increasing concentration will thus lead to more polyelectrolyte molecules available for adsorption to the film during the short droplet contact time.

Interestingly, the film thickness increases with PAA solution concentration until 80 mmol concentration, where the film thickness reaches a maximum value and flattens out. This maximum value of film thickness is due to the electrostatic nature of the LbL process. Films are deposited using electrostatic interactions between the substrate and the two oppositely charged polyelectrolytes. As a charged surface is exposed to the oppositely charged polyelectrolyte solution the polymer chains adsorb to the surface building a layer. After enough of the polyelectrolyte chains have adsorbed, the surface experiences a charge reversal. If the surface is exposed to enough polyelectrolyte, the charge reversal will be strong enough to prevent other liked charged polyelectrolytes from adsorbing to the surface. This is the point of polyelectrolyte saturation on the film surface layer. For the PAH/PAA films studied here, this saturation point occurred at a PAA concentration of 80 mmol resulting in a 25 bilayer film thickness of approximately 600 nm. The film thickness did not increase past 600 nm with any further increase in PAA concentration. This same trend is observed when using the dipping technique to deposit films. Figure 3 demonstrates that dipped films also increase with PAA concentration to a maximum value, and then experience a plateau in film thickness near a concentration of 80 mmol. This indicated that Spray-LbL technique is an electrostatic controlled adsorption process.

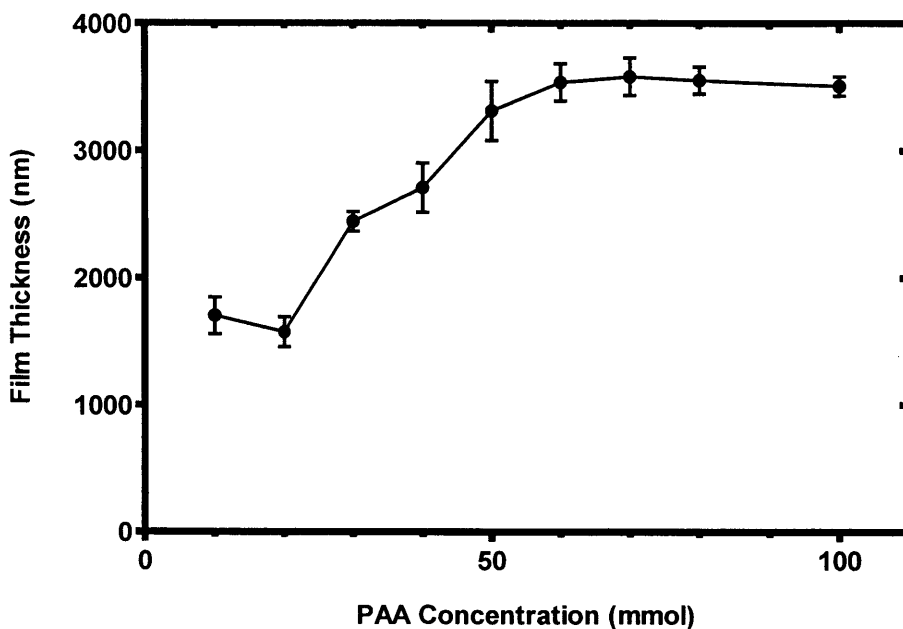


Figure 3. Correlation of film thickness to PAA concentration by dipping.

For (PAH/PAA)₂₅ films deposited by the traditional dipping LbL technique. Film thickness increases with concentration up to a maximum possible thickness between 70 - 80 mmol concentration. Due to the small size of the dipped samples, thickness measurements could not be obtained with the ellipsometer.

For the automated Spray-LbL system, the film thickness reaches a maximum value at a PAA concentration of 80 mmol; however, the film roughness does not seem to level off at this concentration, but instead continues to increase significantly as shown in Figure 4. Focusing on the roughness data between 10 and 80 mmol PAA concentration, the minimum RMS value is 59.4 Å (at 50 mmol) and the maximum RMS value is 151.6 Å (at 60 mmol). The film roughness almost triples with a 10 mmol increase in concentration. However, below 50 mmol concentration the RMS values do not differ by more than 20 Å. To obtain the smoothest possible films, concentrations of 50 mmol or less should be used.

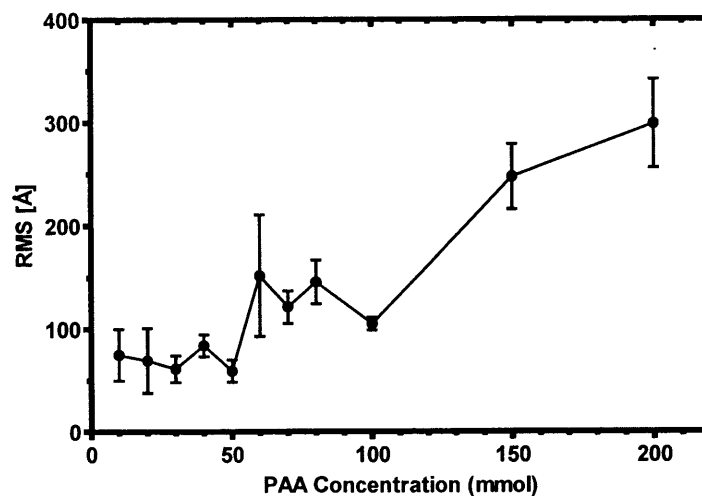


Figure 4. Correlation of film roughness to PAA concentration.

For the (PAH/PAA)₂₅ system deposited by the automated Spray-LbL technique.

Regarding film thickness, there is no benefit to using solutions in excess of 80 mmol of PAA. However, at concentrations less than 80 mmol for the other standard parameter values it is possible to make significant adjustments to film thickness by altering the PAA solution concentration. The roughness data shows that using solutions greater than 50 mmol will result in a sizeable increase in roughness. The reason for this increase is not clear, but it possibly could be due to concentrations greater than 50mmol causing the individual polymer chains to interact with each other and influence each other before they are exposed to the surface. Concentrations used in Spray-LbL should be kept to 50 mmol or less to produce smooth films. Limiting the solutions concentrations to below 60 mmol will still allow for over 100 nm adjustment to film thickness in 25 bilayer films while maintaining a smooth overall film. Adjusting the concentration of the polyelectrolyte solutions used in the Spray-LbL technique is an effective way to change the thickness of the films produced.

1.3.1.2 Polyelectrolyte Spray Time

Another significant parameter to control film thickness is the spraying time or contact time between the polyelectrolyte and the film surface. Like concentration, the contact time parameter is also found in traditional LbL deposition in the form of dipping time. Increasing the contact time should have a similar effect to that of concentration. Increasing the contact time, will increase the amount of polyelectrolyte available for adsorption to the surface. For this work, the spraying time of the PAA solution was the only parameter adjusted from the standard sample (Table 1) and the spraying time of the PAH solution was held at 4 s. PAA spray time was adjusted from 1 s to 20 s. In this case, increasing the contact time allows more time for the diffusion process through the liquid coating resulting from the droplets impacting the surface. If the exposure time is equal to or greater than the diffusion time of the polyelectrolyte in this liquid surface coating, then the polyelectrolyte chains will be able to diffuse to and adsorb to the surface. Instead of increasing the amount of polyelectrolyte in the droplets, as was done in the concentration study, the exposure of the polyelectrolyte solution was increased, thus increasing the number of chains that diffuse to the surface. The expected trend is easily seen in Figure 5. The point of polyelectrolyte saturation occurs between 10 and 15 seconds of polyelectrolyte spraying time. The films from this investigation do not reach the same exact saturation point that was observed in the concentration investigation as evident by the 25 bilayer film thickness values, 500 nm and 600 nm respectively. This is more than likely due to the absence of the chain to chain influence that was discussed for the highly concentrated solutions.

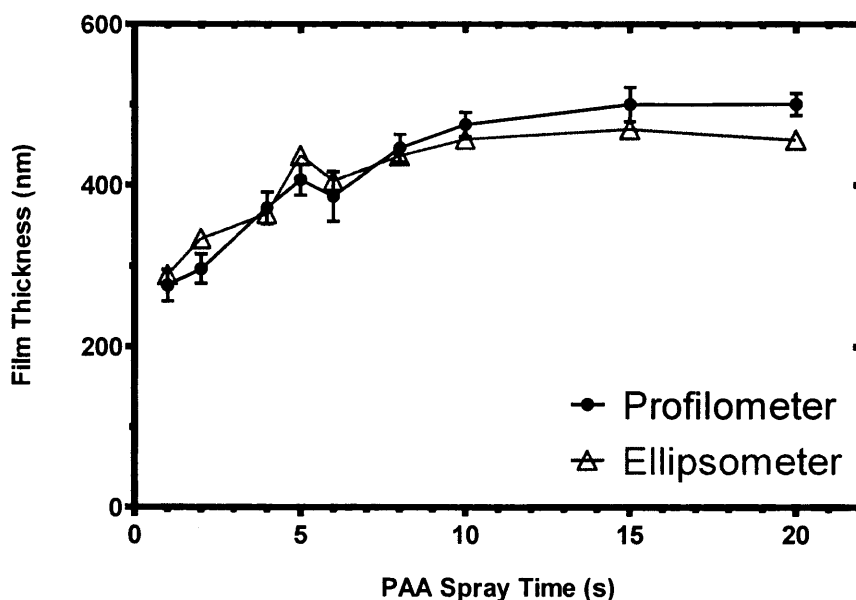


Figure 5. Correlation of film thickness to PAA spray time.

For the (PAH/PAA)₂₅ system deposited by automated Spray-LbL. Film thickness increases with spray time up to a maximum possible thickness that occurs at a spraying time between 10 -15 seconds.

Polyelectrolyte spray time affects the film roughness in a similar manner as it affects film thickness. Figure 6 shows that as spray time is increased, the film roughness also increases up to a maximum value between 10 s, akin to film thickness. However, spraying longer than 6 seconds will result in a more than 200% increase in film thickness for the 25 bilayer films, which is not desirable when looking for smooth films. For a smooth film, a spraying time of less than 6 s should be used.

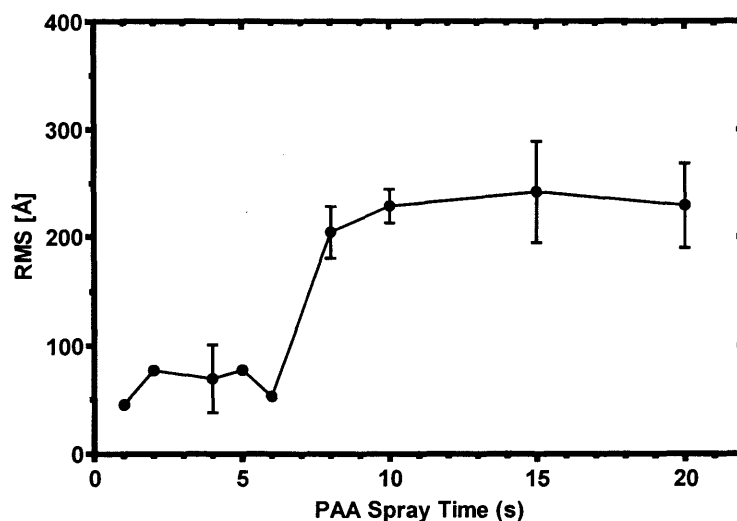


Figure 6. Correlation of film roughness to PAA spray time.

For the (PAH/PAA)₂₅ system deposited by the automated Spray-LbL technique.

These results illustrate a clear correlation between spray time and thickness. Figure 5 shows that beyond 4 s the 25 bilayer film thickness actually increases more than 100 nm before leveling off just beyond 10 s, while Figure 6 shows that beyond 6 s the film roughness more than doubles before reaching the point where thickness levels off. It is possible to adjust the film thickness using the spray time, but to maintain a smooth film all adjusted spray times should be kept to 6 s or less.

1.3.1.3 Spraying Distance

A third parameter that is suited for adjusting film thickness is the distance between the spray nozzles and the substrate. The automated Spray-LbL system uses commercially available airbrushes (Badger Inc.) to produce the polyelectrolyte and rinse sprays. These airbrushes have nozzles that produce a cone of spray droplets. As the distance from the nozzle increases, the diameter of the spray

cone expands. If the substrate is too close to the nozzles, the cone will not be large enough to cover the entire surface. However, if the substrate is too far away from the nozzles then the cone will be much larger than the substrate surface and most of the droplets will not impact the surface. For this work, the spraying distance from the nozzles to the substrate was the only parameter adjusted from the standard sample (Table 1). The spraying distance was adjusted from 5 in to 13 in. At distances less than 5 in, the cone of spray droplets did not cover the entire substrate, and beyond 13 in more than 50% of the spray impacted off of the substrate. Based on these spray cone patterns, the automated Spray-LbL system was originally designed for a fixed distance of 7.5 inches between the nozzles and the substrate.

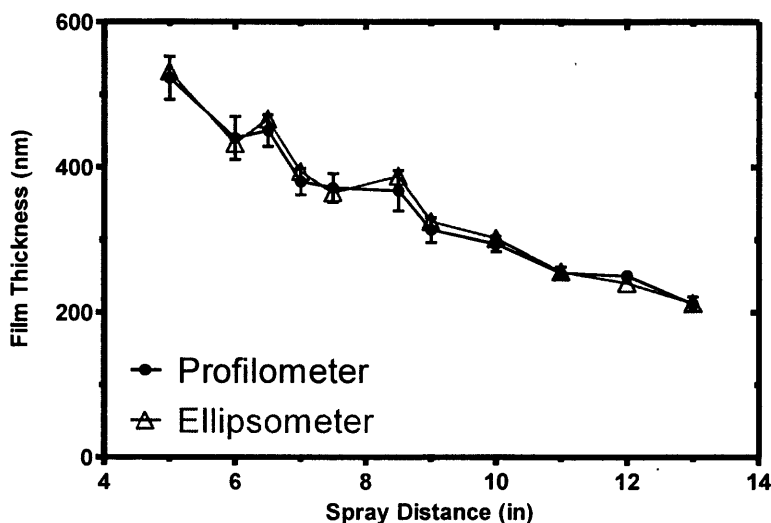


Figure 7. Correlation of film thickness to spraying distance.

For the (PAH/PAA)₂₅ system deposited by automated Spray-LBL.

The trend resulting from adjusting the spray distance is a nearly linear, inverse relationship between distance and film thickness, Figure 7. The film thickness changed by over 40% from one limit to the other. At distances close to the nozzle, more of the droplets are impacting the film surface at one time, which translates to more polyelectrolyte available to adsorb to the surface. As distance increases

the number of droplets impacting the surface decreases, and thus the number of polyelectrolyte chains available near the surface decreases. This effect can be viewed similarly to decreasing the concentration of polyelectrolyte in each droplet; less polyelectrolyte available to bind to the surface will result in thinner films.

Table 2. Impact velocity of the PAA solution droplets at the adjusted spraying distances.

Spraying Distance (in)	Impact Velocity (m/s)
5.0	6.8
6.0	6.2
6.5	5.7
7.0	5.5
7.5	5.2
8.5	5.0
9.0	4.7
10.0	4.0
11.0	3.2
12.0	2.3
13.0	1.4

Another affect of increasing the spraying distance is a decrease in droplet velocity, as seen in Table 2. By increasing the spray distance the droplets must travel further through the ambient environment, increasing the decelerating effects of air resistance, gravity, and droplet collisions. The droplets have a spherical shape as they exit the nozzles and travel toward the substrate, Figure 8a. When the droplets impact with the surface they coalesce and form a thin film of liquid on the surface of the substrate. The thickness of this water film depends on the force of the impact of the droplets, which is a function of the impact velocity of the droplet, Figures 8b and c. Faster droplets will impact with more force, causing the resulting water film to spread out and become thinner, Figure 8c. This water

film deformation will reduce the diffusion length that the polyelectrolyte chains in the water film must cross to reach the surface making it possible for more polyelectrolyte chains to reach the surface during the spray contact time. Thus, by changing the spray distance, we are changing the impact velocity of the droplet and the resulting diffusion length for the polyelectrolyte in the water film at the surface. A shorter diffusion length will result in more polyelectrolyte chains reaching the surface during the contact time, allowing for more adsorption to the surface and thicker layers.

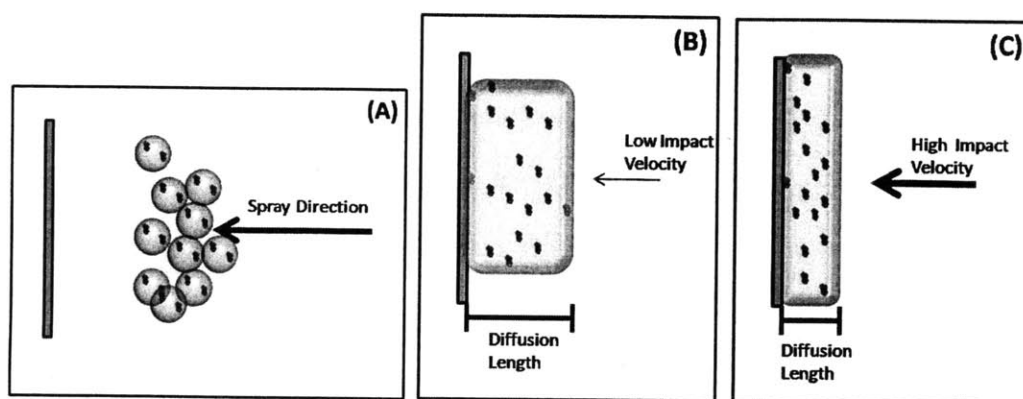


Figure 8. Water film formed upon droplet impact with the surface.

(A) depicts the droplets approaching the surface with a spherical shape. (B) is a depiction of the film of solution formed when low velocity droplets impact and coalesce on the surface. (C) is a depiction of the thin film of solution formed when high velocity droplets impact and coalesce on the surface. This water film is more spread out and thinner.

The observable trend of decreasing film thickness with increasing spray distance is a combination of the two effects of spray distance, the amount of droplets that impact the surface and the force of impact. At close distances, more droplets impact the film surface at one time, as well as

impacting with more force, reducing the diffusion distance. The combination of more droplets and shorter diffusion distances results in thicker films than films made at greater distances.

The roughness measurements based on spray distance are in Figure 9. There is no significant trend observed in roughness. The films are most rough at the extreme values of distance. It seems as if there is an optimal spray cone size to produce a smooth film. If the substrate is too close to the nozzles, the spray cone is too small and the droplets impact with a high velocity and potentially deform or rupture the film surface upon impact. If the substrate is too far from the nozzles, the spray cone is too large and fewer droplets will impact the surface. This could lead to the formation of islands of polyelectrolyte on the surface during the first bilayers, which would result in the rougher films. Between 7.5 – 11 inches, the spray cone is at its optimal diameter, resulting in uniform coverage of the film surface and a regular impact velocity. An in depth study into the mechanics of the spray droplets from the nozzles to the substrate is required to understand what causes this roughness behavior.

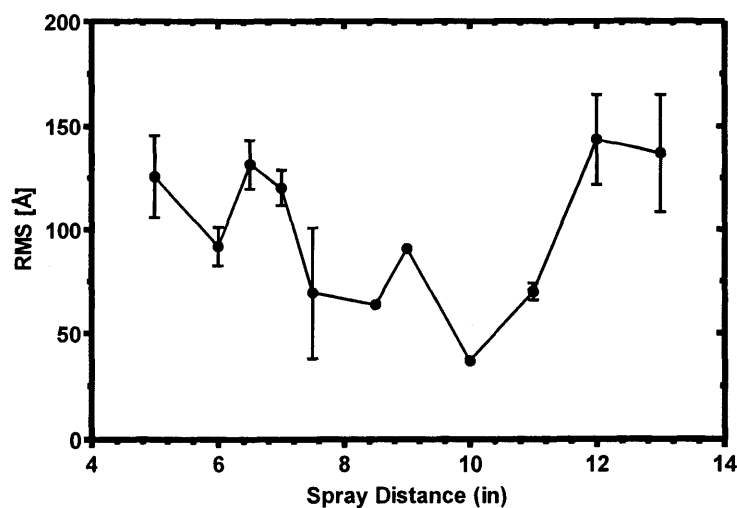


Figure 9. Correlation of film roughness to spray distance.

For the (PAH/PAA)₂₅ system deposited by the automated Spray-LbL technique.

Spraying distance is a simple way to control the thickness of deposited films without changing the solutions or timing setup of the Spray-LBL system. All that is required is moving the substrate closer to or farther from the nozzles. However, if the substrate is too close or too far away, resulting in a much thicker or much thinner film respectively, the film will also become much rougher. As such, care must be taken when adjusting the film thickness outside of the 7.5 in - 11 in range in distances.

1.3.1.4 Air Pressure

The fourth parameter well suited for fine-tuning thin films is the air pressure. The flow of the high pressure nitrogen gas through the inside of the airbrush causes the polyelectrolyte solution to be nebulized into droplets²² and it also determines the velocity that the droplets impact the surface. As the high pressure gas flows past the opening of the polyelectrolyte solution feed tube, the resulting Venturi effect causes the liquid solution to be drawn up into the airbrush nozzle, where it is broken up into droplets²² and expelled out of the nozzle. The exit velocity of the droplets is directly correlated to the air pressure of the compressed nitrogen supply. For this work, the air pressure supplied to the system was the only parameter adjusted from the standard sample (Table 1). The air pressure was adjusted from 10 psi to 35 psi. The velocities corresponding to the air pressure values are listed in Table 3.

Table 3. Exit and impact velocity of the PAA solution droplets at the adjusted air pressures.

Air Pressure (psi)	Exit Velocity (m/s)	Impact Velocity (m/s)
10.0	5.0	2.1
15.0	6.4	3.0
20.0	8.0	3.6
25.0	9.4	5.2
30.0	10.4	5.8
35.0	12.5	6.2

The effect of droplet velocity on film thickness was previously discussed in the spraying distance investigation. To summarize, increasing the droplet impact velocity will cause the droplet to deform at impact and reduce the diffusion length for the polyelectrolyte chains inside. This will result in more polyelectrolyte chains reaching the surface during the set contact time, and thus a thicker film. While the impact velocity of the droplets will always be less than the nozzle exit velocity, due to air resistance, gravity and droplet collisions, the two velocities will be correlated as seen in Table 3. If the exit velocity is increased, the impact velocity of the droplet should also increase, which will result in a thicker film. This trend is seen for the range of air pressures in Figure 10.

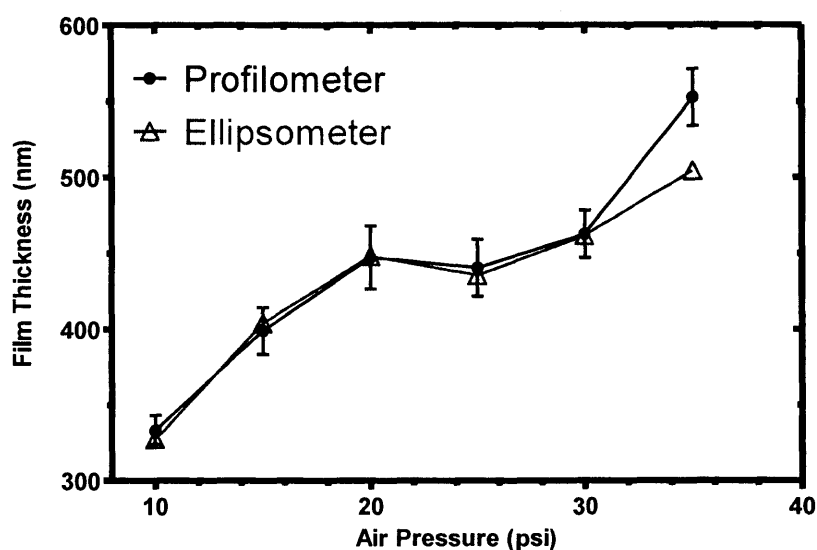


Figure 10. Correlation of film thickness to air pressure.

For the (PAH/PAA)₂₅ system deposited by automated Spray-LBL.

Film roughness also increases with increasing pressure, shown in Figure 11. This increase in roughness, as with the spray distance, seems to be related to impact velocity. The smoothest film is found at the lowest pressure, and the roughness continues to increase as the air pressure is increased.

Table 3 shows a direct correlation between air pressure and droplet impact velocity. The faster impact velocities most likely cause the film surface to deform as the droplets impact, leading to increased film roughness. In order to minimize roughness, the lowest possible air pressure should be used.

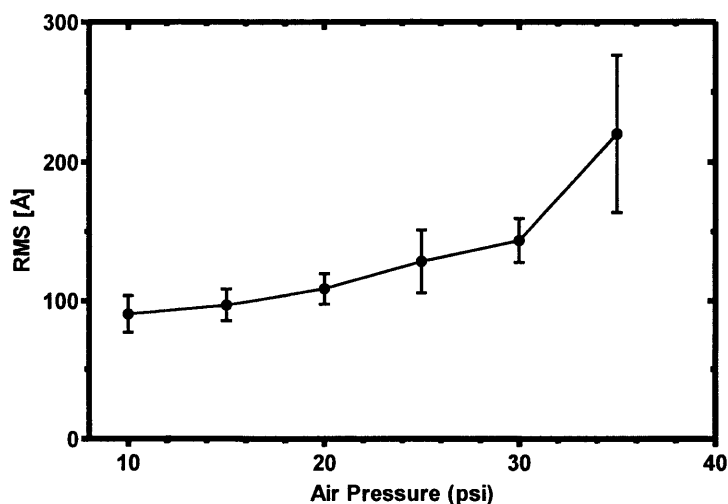


Figure11. Correlation of film roughness to air pressure.

For the (PAH/PAA)₂₅ system deposited by automated Spray-LBL.

Increasing the air pressure will increase the droplet impact velocity resulting in a shorter diffusion length for the polyelectrolyte chains in the droplets and a thicker, but rougher film. Both film thickness and roughness have a direct relationship with air pressure; increasing the air pressure will increase both the film thickness and film roughness. It is possible to adjust the 25 bilayer film thickness by over 200 nm between air pressures of 10 psi and 35 psi, but the film roughness also changes by over 130 Å over this range of air pressures. Like spraying distance, air pressure is another simple way to control film thickness without significant changes to the spray system or solutions used.

1.3.1.5 Polyelectrolyte Charge Density

The final parameter well suited to control the film thickness is the polyelectrolyte charge density. Similar to solution concentration and contact time, charge density is a operational parameter also found in the traditional dipping process. The charge density along the polyelectrolyte chain will determine the chain shape at deposition. Polymers with a low charge density will have a coiled shape, as it is entropically favored for these long chains to fold up rather than lie flat, and the low charge density has a minimal effect on this entropic conformation. However, in high charge density chains, the chain actually repels itself and tends to form a more extended and flat shape.²³ The charge density of a chain is determined by the pH for weak polyelectrolytes and by the screening effect of salt in the solution for strong polyelectrolytes. Both PAH and PAA are weak polyelectrolytes, so their charge density is determined by the solution pH. Many extensive studies have been conducted to investigate the effect of pH on multilayered thin films^{3, 20}, so the effects of pH are widely accepted. It has also been shown that the films produced from Spray-LbL are comparable to those produced by traditional LbL. As such, the effects of pH in (PAH/PAA)_n films are well documented³ and not extensively investigated here. To confirm the expected results, the pH of the PAA solution was the only parameter adjusted from the standard sample (Table 1). The PAA solution pH was adjusted from 6.0 to 8.0. The standard sample film was chosen at pH values near each of the polyelectrolytes' pKa values, 8.8 for PAH and 6.5 for PAA²⁰, which means that both polyelectrolytes are at roughly 50% charge density and will have a coiled shape. This work confirms the trend seen by Shiratori and Rubner³ when adjusting the PAA pH, see Figure 12.

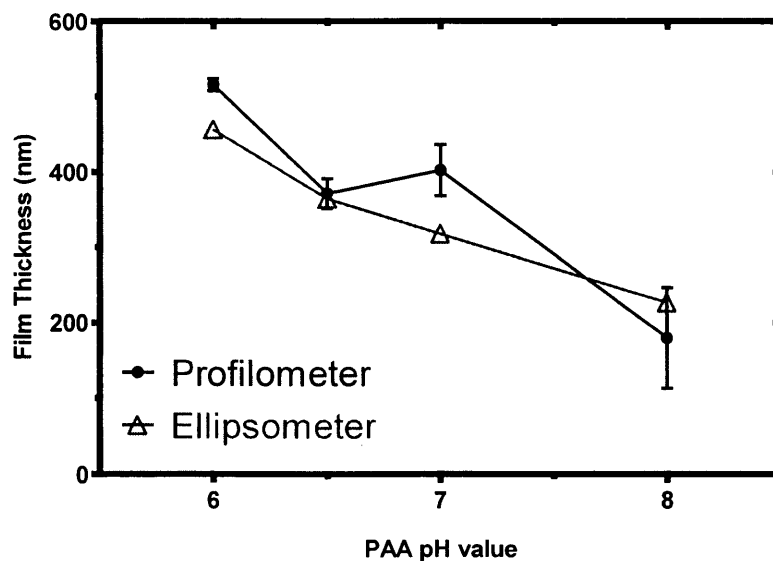


Figure 12. Correlation of film thickness to PAA pH.

For the (PAH/PAA)₂₅ system deposited by automated Spray-LBL.

Decreasing the pH of the PAA causes the PAA chains to have less charge density, resulting in a more coiled, globule-like shape. This means that each PAA chain will be able to occupy less binding locations on the film surface, since some of its negative charge density will be located inside the coiled shape and unavailable for electrostatic binding with the film surface. Hence, more PAA coiled chains will be able to adsorb to the total film surface, and their thicker shape will result in a thicker layer and thicker total film. Alternatively, increasing the pH of the PAA solution will increase the charge density on the PAA chains, causing them to repel themselves and take an extended shape. As these extended polymers adsorb to the surface, they will have more negative charge exposed and available for binding. As such, fewer PAA chains will be able to adsorb to the total film surface resulting in a thinner layer of PAA and a thinner total film. These results follow the expected trend. It was discovered that the film produced with partially charged polyelectrolytes were much thinner when sprayed than dipped due to

interdiffusion of the PAH in the dipped films. This interdiffusion phenomenon is discussed extensively in Chapter 2.

While modifying the polyelectrolyte charge density can have a significant effect on film thickness, Figure 13 shows that there is little change in film roughness when the pH is changed. The film roughness remains nearly unchanged (57.8 Å, 69.25 Å, 59.1 Å, and 57.6 Å) over this range of PAA pH values.

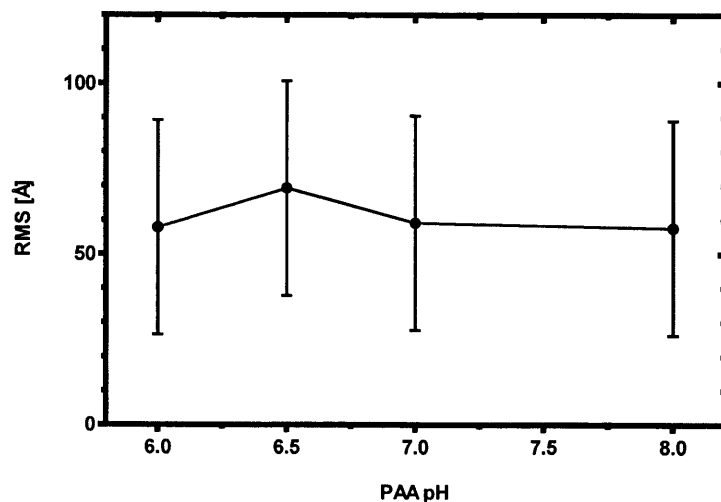


Figure13. Correlation of film roughness to PAA pH.

For the (PAH/PAA)₂₅ system deposited by automated Spray-LBL.

Adjusting the charge density on one of the polyelectrolytes used in the automated Spray-Lbl process can have a significant effect on the film thickness while leaving the film roughness virtually unchanged. For the pH range chosen, it is possible to change the 25 bilayer film thickness by over 330 nm while changing the film roughness by less than 5 Å. The effect of pH adjustment in (PAH/PAA)_n films is well understood and documented³ for traditional LBL and for the most part the films deposited using

automated Spray-LBL follow the same trends, making this an effective parameter if an adjustment in film thickness is needed without changing film roughness or using additional polyelectrolyte.

1.3.2 The Effects on Film Thickness of the Other Parameters

The remaining 5 parameters do affect the film thickness; however, the correlations are not as strong as the optimal parameters listed previously. These should not be the parameters chosen to adjust the film thickness or roughness, but they can be used to do so if necessary. While they are not optimal for adjusting thickness, the effects of these 5 parameters still need to be examined.

1.3.2.1 Molecular Weight

The molecular weight of the polymers will have an effect on the size of the films deposited. For this work, the molecular weight of the PAA was the only parameter adjusted from the standard sample (Table 1). The PAA molecular weight was adjusted between values of 1,200 Da, 15,000 Da, 345,000 Da, and 1,250,000 Da. These molecular weight values were chosen because solutions of PAA with these molecular weights were readily available for purchase at a low cost. The resulting thicknesses for each PAA molecular weight are shown in Figure 14. The most significant result from these experiments is the ability to spray very large molecular weight polymers. Prior to this study, the largest possible molecular weight that could be sprayed without clogging the nozzles was thought to be 400,000 Da. However, this work demonstrated that it is possible to spray low concentrated solutions of polymers with molecular weights in excess of 1 million Da. This is significant as the scope of the automated Spray-LBL process is expanding to incorporate larger and more complicated species. Now, even larger species can be utilized

for Spray-LbL. The molecular weight is also helpful in further limiting the interdiffusion of the partially charged PAH in this system, which is discussed in extensive detail in Chapter 2.

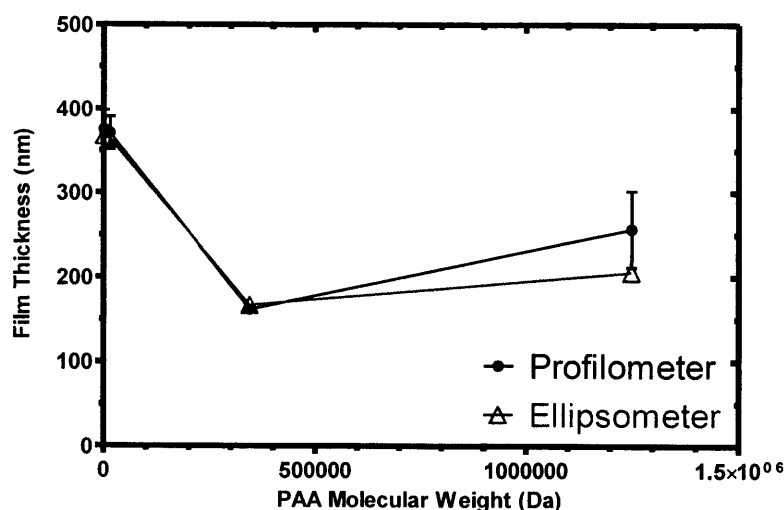


Figure 14. Correlation of film thickness to PAA molecular weight.

For the (PAH/PAA)₂₅ system deposited by automated Spray-LBL.

The effects of molecular weight on film roughness are also ill defined based on this work. Due to the large steps in molecular weight values available, it is hard to determine a noticeable trend from the data shown in Figure 15. As expected, using the extremely large 1,250,000 Da PAA led to much rougher films than the other molecular weights of PAA, but the large difference in molecular weights make it difficult to determine what is happening to roughness between these data points. Focusing on the first three molecular weight values of 1,200 Da, 15,000 Da, and 345,000 Da, the resulting film roughness are 55.33 Å, 69.25 Å, and 28.80 Å respectively. The 345,000 Da PAA is smoother than the smaller molecular weights because of its hindrance of the interdiffusion phenomenon discussed in Chapter 2.

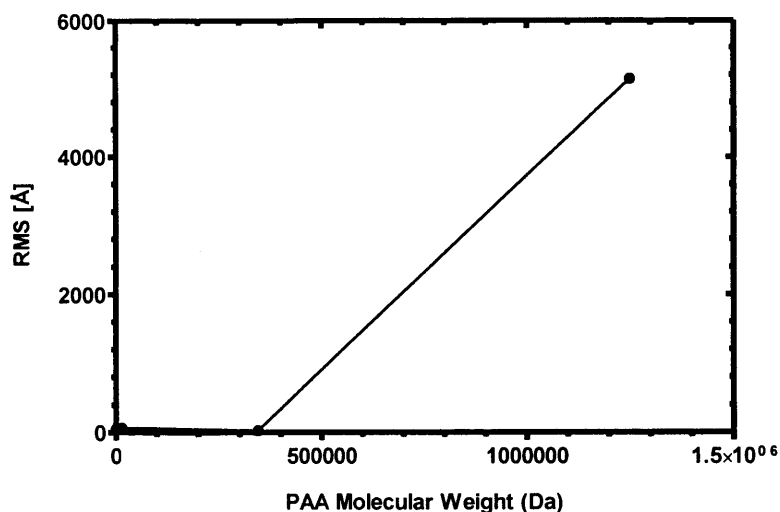


Figure 15. Correlation of film roughness to PAA molecular weight.

For the (PAH/PAA)₂₅ system deposited by automated Spray-LBL.

Changing the molecular weight affects the film thickness, most notably by limiting the interdiffusion in the film. In this setup the larger PAA molecules, 345,000 Da and higher, hinder interdiffusion leading to thinner and smoother films. However, in a polyelectrolyte system with no interdiffusion, the film behavior based on polyelectrolyte molecular weight should be similar to the effects seen here for the molecular weights of 345,000 and 1,250,000 Da. Increasing the molecular weight would increase the thickness and roughness of the film if interdiffusion was not a factor. Because of the limited number of cheaply obtainable PAA molecular weights, only a few widely dispersed molecular weights, some with interdiffusion and some with very limited interdiffusion, were available for this work making it very difficult to identify trends in the data.

1.3.2.2 Number of Airbrush Turns

The number of airbrush turns does have an effect on film thickness; however, it can have an adverse effect on film roughness. The number of airbrush turns controls the liquid to air ratio in this automated Spray-LbL system. An internal needle runs the length of the airbrush and is connected to a knob at the rear, allowing the needle to be moved in and out of the airbrush. The needle covers the top of the liquid feed tube inside the airbrush. When the needle is fully inserted into the airbrush, it completely covers the feed tube opening, preventing any of the liquid from entering the airbrush. As the needle is moved back out of the airbrush, the opening at the top of the feed tube is uncovered, allowing the liquid to be drawn into the airbrush nozzle due to the Venturi effect produced by the high pressure gas flowing through the airbrush. The further back the needle moves, the more liquid is able to enter the airbrush, thus increasing the liquid to air ratio and increasing the amount of liquid sprayed. The number of turns was determined by counting the number of full turns of the needle knob from the completely closed position. For this work, the number of turns on the PAA airbrush was the only parameter adjusted from the standard sample (Table 1). The number of turns was adjusted from 2 to 7. At 1 turn the needle covered too much of the feed tube preventing any liquid from entering the nozzle, and beyond 7 turns the flow rate remained the same. The resulting PAA solution flow rates were determined and are listed in Table 4.

Table 4. Flow rate of the PAA solution for each value of airbrush turns.

Number of Airbrush Turns	PAA Flow Rate (ml/s)
2.0	0.050
3.0	0.150
4.0	0.200
5.0	0.325
6.0	0.350
7.0	0.400
8.0	0.400

The effects of the PAA number of turns on film thickness are shown in Figure 16. Increasing the number of turns, which increases in the liquid to air ratio, resulted in more liquid being sprayed producing thicker films. This relationship is similar to that observed when adjusting the PAA concentration and spray distance, by having more polyelectrolyte available to adsorb to the surface, we are able to produce thicker films.

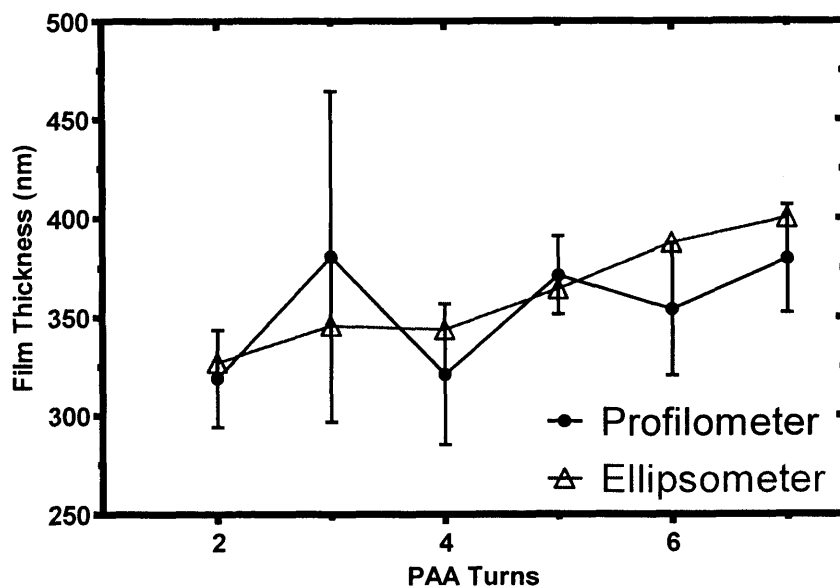


Figure 16. Correlation of total film thickness to PAA airbrush turns.

For the (PAH/PAA)₂₅ system deposited by Spray-LBL.

However, the number of turns has no significant effect on roughness as seen in Figure 17. The large errors in each of these measurements make trend identification difficult. It appears that 3 or 4 turns produce the smoothest film, but the error makes that more of a speculation than a valid observation.

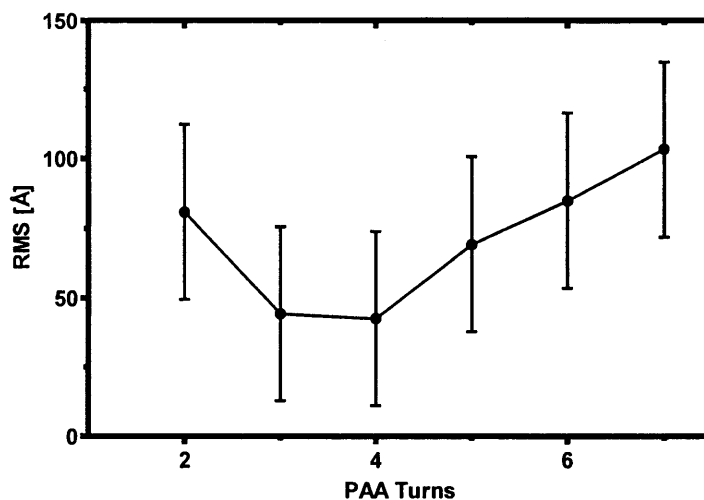


Figure 17. Correlation of film roughness to PAA airbrush turns.

For the (PAH/PAA)₂₅ system deposited by automated Spray-LBL.

The film thickness has a direct relationship with the number of airbrush turns or liquid-to-air ratio. Increasing the number of turns will increase the film thickness; however, the film roughness has no significant trend.

1.3.2.3 Rinse Time

The rinse spraying time is another operational parameter of the automated Spray-Lbl system. After each polyelectrolyte deposition and drain step, the film is rinsed with water to remove polyelectrolyte chains that form very weak bonds with the film surface. When polyelectrolyte chains adsorb to the surface, the strength of the electrostatic binding is a result of the number of electrostatic bonds formed between the chain and the surface. The more bonds that form, the stronger the overall bond between the polyelectrolyte chain and the surface. Chains with only one or two bonds will be very

weakly bound to the surface and can affect the quality and strength of the film. It is desirable to eliminate these weakly bound chains, which is why the rinse step is needed. Rinsing is very important in dipped LbL to produce good quality films. As such, the rinsing steps were originally designed into the Spray-LbL process because it was thought they were vital to LbL. However, work by Izquierdo and co-workers has suggested that the rinsing step is not necessary in Spray-LbL, because the shear forces on the film surface and the droplets drain off of the surface will remove the loosely bound polyelectrolytes.¹⁷ They propose that the rinsing step can be eliminated as long as adequate draining of each polyelectrolyte is allowed to occur. To validate the necessity of the rinse step, and look at the effect of the rinse time, the rinsing times were the only parameter adjusted from the standard sample (Table 1). The rinse times were adjusted from 0 s - 20 s. The draining time for the polyelectrolytes remained constant at 5 s. Figure 18 clearly shows that the rinse step is needed, if the draining time is not adjusted. The film produced with no rinse was more than twice as thick as any of the rinsed films. However, the films produced with varying rinse times had very little variation in film thickness after 2 s. There was an increase of only 29 nm in the 25 bilayer film thickness between the films produced with 1 s rinse time and 2 s rinse time. Beyond 2 s, the thickness slightly decreased by less than 20 nm. These results do show that the rinse is important, contrary to the work of Izquierdo, but the time of rinsing has very little effect on thickness. Currently, 10 s is the accepted rinsing time for this automated Spray-LbL system, but this work suggests that the rinse time could be reduced down to 2 seconds with almost no difference in the films produced; allowing for an even shorter deposition time.

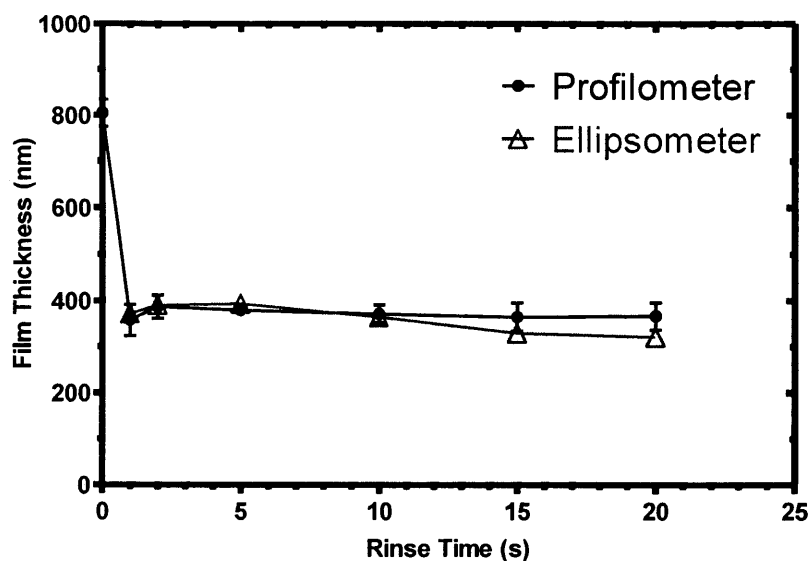


Figure 18. Correlation of film thickness to rinse time.

For the (PAH/PAA)₂₅ system deposited by automated Spray-LBL.

Rinsing time had a very similar effect on roughness. Figure 19, shows that with no rinse the film is more than double the thickness of the rinsed films. And, once a rinse is applied with at least 1 s, the films become smooth with little variation in roughness as rinsing time increases. The film produced at 15 s rinse time appears smoother than the other films, but it is within experimental error of the flat roughness trend of the other rinse times. Similarly to what was observed in film thickness, the roughness is relatively unchanged beyond 1 second of rinse time. This also shows that the rinsing time can be reduced from the standard 10 s to 2 s with very little effect on the film. This reduced rinse time would make automated Spray-LbL even faster; reducing the bilayer deposition time from approximately 60s closer to 30s.

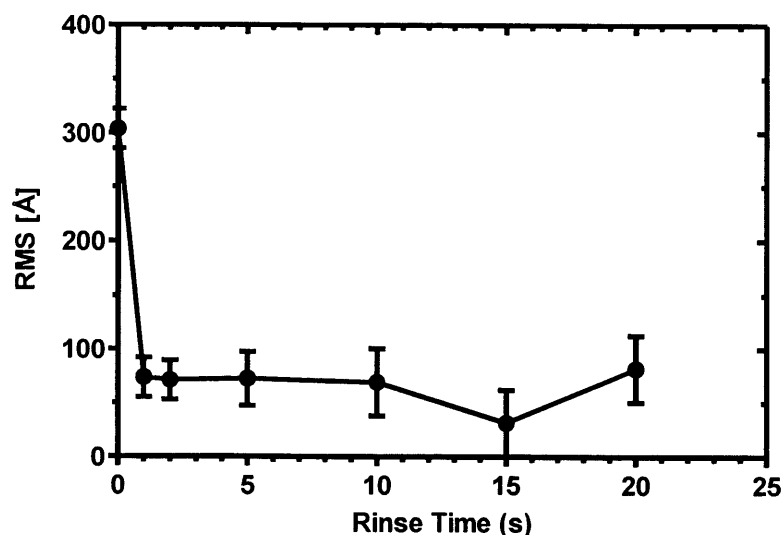


Figure 19. Correlation of film roughness to rinse time.

For the (PAH/PAA)₂₅ system deposited by automated Spray-LBL.

The rinse step is important to the automated Spray-LbL process. It makes the films much smoother and thinner. However, there is little difference in thickness and roughness between films made with a 1 s rinse and those with a 20 s rinse. Rinsing is vital, but the length of rinse has a very slight affect on the films produced.

1.3.2.4 Additional Solvents

Another parameter investigated to control film thickness was the addition of another solvent to the polyelectrolyte solution. For this work, two solvents, ethanol and tetrahydrofuran (THF), were added to the aqueous PAA solution. These solvents were added individually to the PAA solution to yield solutions with 0%, 5%, 10%, 20%, 30%, 40% and 50% of the additional solvent. The resulting thickness values are shown in Figure 20. In figure 20a, as more ethanol is added to the PAA solution the thickness

increases until reaching a maximum value at 20% ethanol in the solution. After 20%, the film thickness begins to decrease. As the ethanol content increased the visible quality of the films changed. During the deposition process, the droplets containing ethanol did not mix well with the layer of rinse water coating the film surface at the start of each PAA spray cycle. With increased ethanol percentage this affect became more visibly obvious. It was also easy to tell which films were made with ethanol in the solution, as the optical Newton rings typically observed in these films were not well defined and seemed to bleed into one another. As shown in Figure 20b, films were only able to be deposited with a maximum of 10% of THF in the PAA solution. Beyond 10% THF, the PAA precipitated out of solution and could not be sprayed. The film thickness does increase with the addition of THF, so adding THF to the polyelectrolyte solutions is a possible option to increase film thickness. Addition of different solvents is not typical in LbL deposition. It would be possible to manipulate thickness with additional solvents, but is not common practice. When adding solvents care should be taken in respect to flammability. By nebulizing the solutions into a fine mist, and using electrical solenoids, the possibility of igniting flammable solvents is greatly increased over the traditional LbL process.

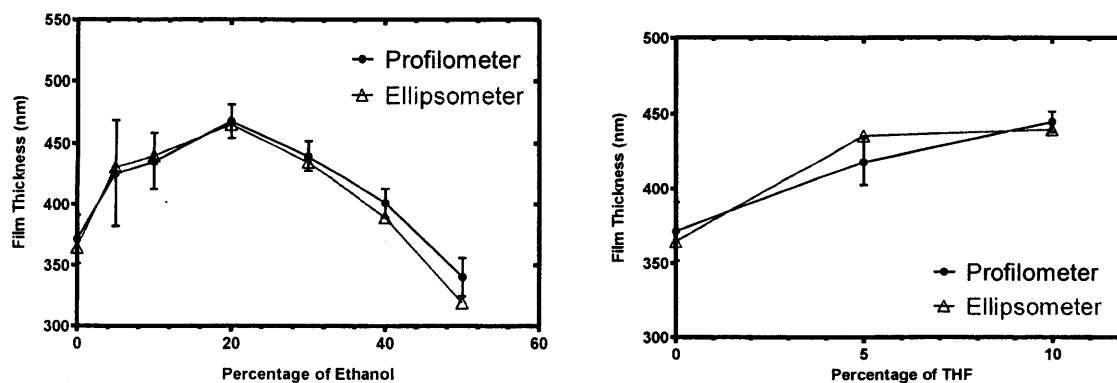


Figure 20. Correlation of total film thickness to the additional solvent added to the PAA solution.

For the (PAH/PAA)₂₅ system deposited by automated Spray-LbL. (A) shows the effects of ethanol. (B) shows the effects of THF.

The addition of solvents to the polyelectrolyte solution has a similar effect on the roughness of the resulting films. Figure 21 shows the roughness values for the films produced when adding ethanol and THF. The addition of ethanol seems to cause a similar behavior in roughness as it did in thickness, with the roughest film occurring at 20% ethanol in solution. The addition of THF also affects the roughness. It seems to lead to an increase in roughness beyond 5%.

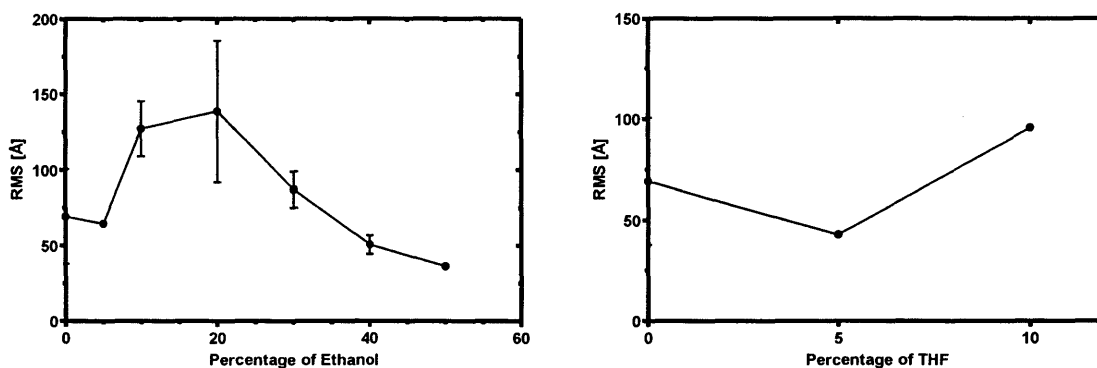


Figure 21. Correlation of film roughness to the additional solvent added to the PAA solution.

For the (PAH/PAA)₂₅ system deposited by automated Spray-LBL. (A) shows the effects of ethanol. (B) shows the effects of THF.

While adding ethanol to the PAA solution seems like a valid way to increase the thickness, it also causes an increase in film roughness. However, using co-solvents is not common practice in layer by layer, and due to the fact that the roughness and thickness behave in the same manner, adding different solvents is not the best option for fine-tuning the film.

1.3.2.5 Number of Bilayers

The final operational parameter of the Spray-LbL process is the number of bilayers in the film. The number of bilayers has a very logical affect on the film thickness; increasing the number of bilayers

increases the film thickness, shown in Figure 22. Typically, LbL film thickness grows linearly with the number of bilayers, except in cases where polyelectrolyte interdiffusion results in an exponential growth regime.¹⁹ In this work, the polyelectrolytes are deposited near their pKa values, which means that both the PAH and PAA are partially charged. These films clearly exhibit exponential growth, as evident from Figure 22. This interdiffusion is discussed in Chapter 2.

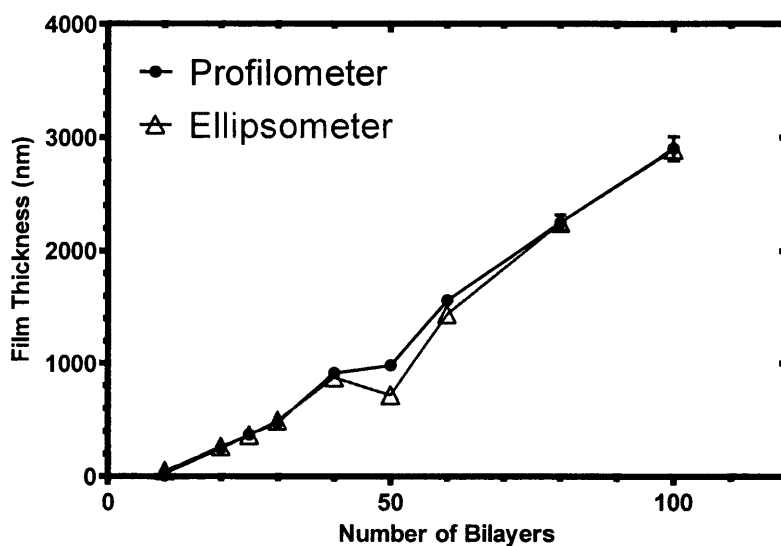


Figure 22. Correlation of total film thickness to the number of bilayers.

For the (PAH/PAA)₂₅ system deposited by Spray-LbL.

Increasing the number of bilayers causes the thickness to increase, and also typically leads to increasing the roughness of the film. Figure 23 shows that this trend is true, the roughness increases with increasing number of bilayers. There is a slight jump in roughness with the 60 bilayer film; however, it is still within error values of the range other values. Adding more bilayers will increase the roughness of the film, if no other changes are made to the automated Spray-LbL system.

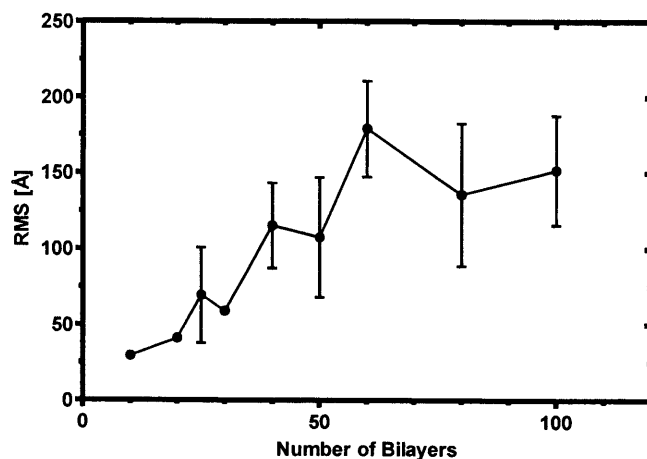


Figure 23. Correlation of film roughness to the number of bilayers.

For the (PAH/PAA)₂₅ system deposited by automated Spray-LBL.

The effect of increasing the number of bilayers is that the film thickness and roughness increase. Adjusting the number of bilayers will easily result in thinner or thicker films, but the film roughness follows the same trend. With the other operational parameters, there was a maximum possible thickness dictated by either the electrostatic interactions or the limits of the parameters themselves. However, there is really no limit to the number of bilayers that can be added to a film, so theoretically there is no limit to film thickness by adding bilayers. Using the automated Spray-LBL system to make an extremely thick film of 600 hundred of bilayers would be possible in approximately 10 hours, whereas the same films would require days approximately 300 hours or 12.5 days. Clearly, ultra thick films would be difficult to make using traditional LBL, but could easily be made using automated Spray-LbL in less time than a 25 bilayer dipped film.

1.4 Conclusion

Of the 10 parameters that can be controlled in the automated Spray-LBL system, 5 parameters generate an evident trend on the thickness of the films produced. These optimal parameters for adjusting film thickness are polyelectrolyte concentration, polyelectrolyte spraying time, spraying distance, air pressure, and polyelectrolyte solution pH. Using the figures in this chapter, it is possible to identify trends in film thickness and roughness for each of the 10 operational parameters. The trends and relationships shown here should hold true for any species combination used in the automated Spray-LBL system, not just (PAH/PAA)₂₅ films. With different species the actual values for film thickness shown in the figures will not be correct, but the trends in those figures will be approximately correct. Thus, if a film made using different species is too thick or too thin, for the most part it would be possible to use this work to determine which parameter will easily change the film thickness enough to produce the desired thickness without making the film too rough. Again, the exact correlations between film thickness and roughness to each parameter will not hold for different species, but the trends for these correlations should.

2. Interdiffusion

Abstract

The interdiffusion of polyelectrolytes during the Layer-by-Layer (LbL) electrostatic deposition process has been shown to produce thin films with superlinear growth in place of the standard linear growth typically observed. The interdiffusion of poly(allylamine hydrochloride) (PAH) in thin films with poly(acrylic acid) (PAA) is investigated using both the conventional dipped LbL and Spray-LbL deposition techniques. Interdiffusion is shown to be dependent on a combination of factors, in particular: the charge density of the polyelectrolytes, their molecular weights, and the contact time between the

polyelectrolyte solutions and the surface of the film. Only when PAH is partially charged (pH greater than 8) is interdiffusion observed. The rate of interdiffusion was molecular weight dependent, suggesting scaling appropriate to macromolecular diffusion, and interdiffusion was primarily observed with LbL systems for which the polyelectrolyte chains were low molecular weight for the contact times and processing conditions of this study. Importantly, the contact time must be long enough to allow interdiffusion to occur; the significantly reduced contact time introduced during Spray-LbL compared to dip-assembly not only speeds up the film deposition time, but also significantly decreases the interdiffusion of PAH, resulting in much thinner films than observed from dipping at the pH conditions for which interdiffusion occurs. The effect of concentration variation in both deposition techniques is also investigated. It is established that dipped films can be as much as an order of magnitude thicker than sprayed films because of interdiffusion; however, both techniques yield films whose bilayer thickness plateaus at high polyion concentrations of 80 mmol PAA concentration and at a given solution contact time, demonstrating that both techniques are driven by the electrostatic interactions and resultant self-limiting adsorption that enables the build-up of thin films.

2.1 Introduction

The layer-by-layer (LbL) thin film deposition process is an established method to produce highly tunable thin films on the nanometer scale.¹ This process involves sequentially exposing a substrate to oppositely charged polyelectrolytes in alternation in order to construct a multilayer film on the substrate. Typically this process is conducted by dipping a substrate with a surface charge into a weak solution of an oppositely charged polyelectrolyte and allowing the polyelectrolyte chains in solution to diffuse to the substrate surface and form electrostatic bonds with the charged surface. In an effort to reduce the assembly time, a variation of the LbL process has been developed, automated Spray-LbL, which consists of spraying the polyelectrolyte and rinse solutions directly onto a stationary vertical substrate.^{2, 7, 17} Typically, it is thought that in adsorption of polyelectrolytes from dilute solution,

polymer chain segments sample the surface and arrange in conformations that lead to a final film surface conformation, although the rearrangements can be kinetically hindered by the presence of electrostatic charge. In spray-LbL, before the polyelectrolyte chains have time to rearrange on the surface in an attempt to reach equilibrium arrangements², the surface is rinsed and the oppositely charged polyelectrolyte is sprayed uniformly onto the surface, kinetically trapping the polyelectrolyte chains in place on the surface.⁷ Dipped LbL films are generated with adsorption over much longer periods, on the timescale of diffusion; polyelectrolyte chains in the bulk solution must diffuse through the solution and onto the oppositely charged surface. This relatively long diffusion time allows many of the polyelectrolyte chains that reach the surface to rearrange in an effort to reach thermodynamic equilibrium. Although such dipped films do not generally reach a true equilibrium state due to strong electrostatic charge interactions that pin chains to the surface, the longer dipping time does allow for more polyelectrolyte rearrangement on the surface and in the film than Spray-LbL.

Certain LbL systems have been observed to exhibit superlinear film growth in dipped LbL films due to a process of polyelectrolyte interdiffusion within the film.^{19, 24} This interdiffusion phenomenon occurs when one or both of the charged polyelectrolytes absorb into the multilayer thin film rather than simply adsorbing on the top charged surface, yielding excess polyion that complexes with more polyelectrolyte in the next dip cycle. It has been observed that polyions undergo interdiffusion into the multilayer when the polyelectrolyte has a low effective charge density. This situation can be seen with certain weak polyelectrolytes at conditions close to their pKa; whereas strong unshielded polyelectrolytes or weak polyelectrolytes that are fully charged do not undergo this interdiffusion phenomenon.²⁴ In this work, we explore this interdiffusion phenomena using two weak polyelectrolytes (PAH and PAA) at 50% charge and with a range of molecular weights, and two different deposition methods, conventional dipped LbL and Spray-LbL techniques, that enable deposition over very different time scales. We use both profilometry and ellipsometry to compare the resulting film thickness

between the two deposition techniques and Quartz Crystal Microbalance with Dissipation to determine the diffusion time for polyelectrolyte. We find that interdiffusion occurs in films constructed using the weak polyelectrolytes at low degrees of ionization deposited using both techniques, but that it is much more prominent in dipped films. This confirms that the polyelectrolytes are kinetically trapped on the surface upon exposure to the oppositely charged polyelectrolyte, and demonstrates that the timescale of multilayer interdiffusion can take place over the timescale of the spray-LbL deposition process.

2.2 Experimental Section

2.2.1 Materials

Poly (acrylic acid, sodium salt) (PAA, MW=15 000 g/mol, 35% aqueous solution) was purchased from Sigma Aldrich. Poly (acrylic acid) (PAA, MW=345 000 g/mol, 25% aqueous solution) and Poly(ally amine hydrochloride) (PAH, MW = 55 000, powder) was purchased from Polysciences. Polymer solutions were prepared using Milli-Q water at concentrations of 10-, 20-, 30-, 40-, 50-, 60-, 70-, 80- and 100 mmol with respect to the repeat unit. PAH solutions were prepared at a pH of 9.0 and 6.5($pK_a \sim 8.8^{20}$) and all PAA solutions were prepared at a pH of 6.5 ($pK_a \sim 6.5^{20}$) All solution pH adjustment was performed using HCl and NaOH, no additional salt was added to the polyelectrolyte or rinse solutions. Spray-LbL films were deposited on 3-inch coin roll silicon wafers (Silicon Quest International), and dipped LbL films were deposited on similar wafers that had been cut into 1cm x 3 cm pieces. All silicon was cleaned with ethanol and Milli-Q water to hydroxylate the surface. Quartz Crystal Microbalance SiO₂ coated sensors (Q-sense) were cleaned with ethanol and Milli-Q water to clean and hydroxylate the surface.

2.2.2 Deposition

Dipped films were constructed using a Carl Zeiss HMS DS-50 slide stainer. The cleaned substrates were first submerged in the PAH solution for 10 min followed by three, 1 min rinse steps in Milli-Q water. The Milli-Q water was used at its default pH. The substrate was then submerged in the PAA solution and rinsed by an additional three, 1 min rinse steps in Milli-Q water. This cycle was then repeated for the required number of bilayers. After the final rinse step, the substrate was removed from the final rinse bath and dried thoroughly. Using this setup a 25 bilayer film required approximately 12.5 h for complete deposition. Sprayed films were constructed using an automated Spray-LbL system.⁷ Identical polyelectrolyte solutions described above for dip-LbL were used for spraying. All spray solutions were delivered by ultra high purity nitrogen gas (AirGas) regulated to 25psi. The PAH solution was sprayed for 4 s and allowed to drain for 5 s before spraying the rinse solution for 10 s. After 5 s for rinse drainage, the PAA solution was sprayed and rinsed similarly. This cycle was then repeated for the desired number of bilayers. Using this setup a 25 bilayer film required approximately 20.4 min for complete deposition. For samples made for interdiffusion comparisons, untreated Milli-Q water (pH of approximately 5.5) was used for rinsing. For samples made for concentration comparisons, Milli-Q water adjusted to the pH value of the corresponding polyelectrolyte was used for rinsing.

2.2.3 Analysis

Film thickness was measured using a Tencor P16 profilometer to drag a stylus across a scored film to determine the step height. A stylus tip force of 0.5 mg was used to avoid film penetration. Eight measurements from different locations on the film were taken to ensure a good average value of film thickness. All bilayer thicknesses reported were determined by taking the total film thickness and then dividing by the number of bilayers. Thickness measurements were checked using a Woolam XLS-100

spectroscopic ellipsometer. Films were dried in a nitrogen stream prior to measurement. A Quartz Crystal Microbalance with Dissipation from Q-Sense was used to measure the diffusion time for the twenty-first layer of PAA on a previously deposited (PAH/PAA)₂₀ film.

2.3 Results and Discussion

Typically polyelectrolyte thin films exhibit linear thickness growth with increasing bilayers. In some cases, such as partially charged weak PEs, films actually exhibit an exponential thickness growth regime. This growth is due to the diffusion of polyelectrolyte into and out of the film.^{19, 25, 26} It has previously been determined that this interdiffusion phenomenon is often due to one of the PEs interdiffusing through the film.¹⁹ One can consider, for example, a system in which a polycation is the diffusive species. When the film is exposed to the polycation solution, the polycation chains adsorb to the surface as expected in the LbL process; however, if the polycation chains are mobile enough and the film allows for mobility, the polycation chains may diffuse through the top polyanion layer of the film and into the bulk film toward areas of available negative charge density^{25, 26}; or into the film in general based on solubility of the polymer chains in the swollen LbL polyion complex matrix. As these polycation chains move into the film, they can also displace other polyion chains in the film if the exchange produces a more charge favored arrangement.^{25, 26} The interdiffusion process continues until the substrate is removed from the polycation solution, rinsed, and placed in the polyanion solution. The polyanion chains in solution near the surface will complex with the excess polycation chains at and near the film surface to create the next adsorbed “layer”. If the film is exposed to high concentrations of polycation and/or sufficiently long adsorption times, then the mobile polycation chains will be able to diffuse into the film and reach mixture equilibrium within the film before being exposed to the polyanion. As the degree of interdiffusion increases, the bilayer thickness increases, and the growth becomes superlinear due to the

corresponding increased multilayer film thickness, which serves as a reservoir for excess polyion. In general, interdiffusion has been observed for weak polyelectrolytes at lower degrees of ionization, for which the polyion chains are more mobile, and less likely to become kinetically trapped upon adsorption on the oppositely charged multilayer surface. For the PAH/ PAA system, it has been shown that it is the PAH that interdiffuses, but that interdiffusion only occurs when the PAH is partially charged, at a pH of 8 or higher.²⁵ To examine this phenomenon we made 25 bilayer films using both dip and spray deposition techniques, the results of which are found in Table 5. For the polycation, PAH was used at 10 mmol concentration at both pH 6.5 (~90% charged) and 9.0 (~50% charged). For the polyanion, two molecular weights of PAA were used at 10 mmol concentration and a constant pH of 6.5 (50% charged). Untreated Milli-Q water was used for all rinse baths. Films were also prepared using partially charged 20 mmol PAH (pH=9.0) and 20 mmol PAA (pH=6.5) to confirm the interdiffusion phenomenon.

Table 5. Average bilayer thickness of (PAH/PAA)₂₅ films made using different combinations of PAA molecular weights and PAH solution pH values.

All solutions made from 10 mmol solutions with the pH of the PAA solutions kept at 6.5 for all films.

Deposition Technique	PAA Molecular Weight	PAH solution pH=6.5	PAH solution pH=9.0
Spray-LbL	15 000	No Films Deposited At These Conditions	7.06 +/- 0.50 nm
Spray-LbL	345 000		3.72 +/- 0.12 nm
Dip LbL	15 000	5.93 +/- 1.13 nm	43.62 +/- 1.27 nm
Dip LbL	345 000	4.99 +/- 0.35 nm	16.98 +/- 2.70 nm

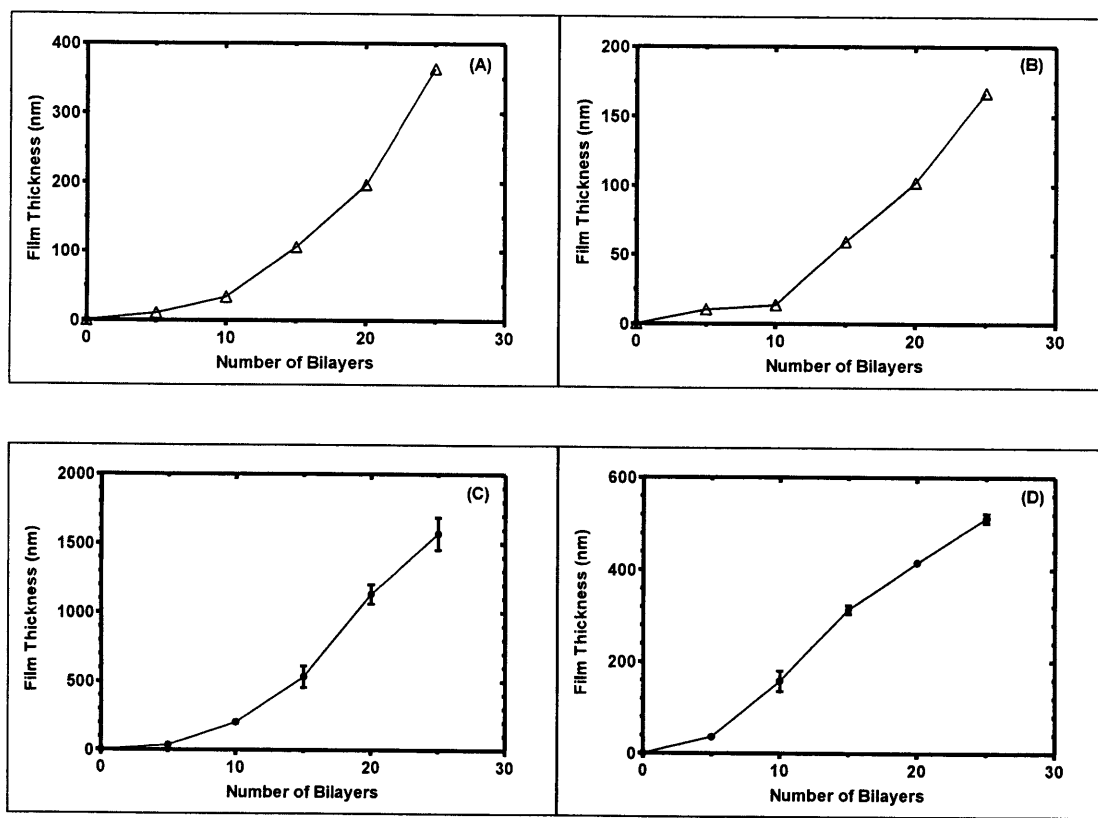


Figure 24. Growth curves for sprayed and dipped (PAH/PAA)₂₅ films. All films deposited with 20 mmol solution concentrations, PAH pH=9.0 and PAA pH=6.5 (A) The sprayed film of 15k MW PAA shows clear exponential growth, indicating interdiffusion is occurring. (B) The sprayed film of 345k MW PAA has an initial exponential growth, but it becomes more linear after 15 bilayers, indicating that interdiffusion occurs, but is not as prevalent in this film. (C) The dipped film of 15k MW PAA shows exponential growth, again indicating interdiffusion is present. (D) The dipped film of 345k MW PAA has relatively linear growth after the first 5 layers are deposited, indicating diffusion is not prevalent in this film.

Examination of film growth behavior and film thickness of the dipped films clearly indicates that the interdiffusion phenomenon occurs as expected. Film bilayer thicknesses at different conditions are shown in Table 5, and the growth curves are found in Figure 24. Interdiffusion is marked by increased

bilayer thickness relative to the linearly growing films and a superlinear growth curve. When PAH is nearly fully charged (pH=6.5) interdiffusion does not occur when paired with either molecular weight PAA solution. In fact, both the 15k and 345k molecular weight PAA films have nearly the same bilayer thickness, 5.93 nm and 4.99 nm respectively. Since the PAH chains are nearly fully charged, they are in an extended conformation and will have a higher positive charge density available for binding to the underlying layer than a less charged polymer chain^{20, 23, 27}. These more highly charged chains are able to form greater numbers of ionic crosslinks within the film, and they adsorb to form more two dimensional conformations on the surface, leading to thinner bilayers. The greater availability of charged binding sites hinders the mobility of the PAH chains in two ways: the increased ionic crosslinking leads to a matrix with a smaller effective mesh size or gap size between linkages, and the high charge density of PAH in the presence of a highly negatively charged PAA surface makes it difficult for PAH chains to move beyond the surface layer and interdiffuse into the film due to the many ionic contacts on the surface that kinetically prevent interdiffusion. However, when the PAH chains are only partially charged (pH=9.0), the charge density along the backbone is much lower, and interdiffusion becomes apparent if the partially charged PAH is paired with the lower molecular weight PAA. When paired with the higher molecular weight PAA, interdiffusion over the deposition timeframe examined here (10 minutes) is not significant. At pH=9.0 the PAH chains will only be partially charged, resulting in a thicker film and chains with a loopier chain conformation.^{20, 23} Because there is less positive charge density for binding locations, PAH chains are less strongly bound to the surface, and become much more mobile, enabling diffusion through the bulk film. However, interdiffusion appears to be inhibited by the size of the PAA chains; this dependence on the molecular weight of PAA implies that PAA chain interdiffusion may also be taking place during the adsorption cycles, or that the ability of polycation chains to diffuse is in part dependent on the mobility of the polyanion chains in the matrix due to the cooperative nature of chain diffusion. In fact, poly(acrylic acid) has itself been known to undergo interdiffusion²⁸ when its charge

density is relatively low. It is also possible that the size of the higher molecular weight PAA chains form denser or more entangled or interconnected networks in the LbL film, limiting the mobility of the PAH chains within the film, impeding the PAH interdiffusion into the film, and thus producing much thinner films than those using the shorter PAA chains. Presuming that chain diffusion occurs in the multilayer film as predicted by simple polymer diffusion models, the diffusivity of the polymer chains is dependent on molecular weight with a power law expression. For this reason, the rate of interdiffusion of larger polymer chains is greatly decreased and interdiffusion is significantly slowed. The combination of the partially charged PAH and shorter, though highly charged, PAA chains yield a film with a bilayer thickness of approximately 43 nm. Using the longer PAA chains produces a film with a bilayer thickness of approximately 17 nm.

While interdiffusion occurs as expected in the dipped films, it is much less prevalent in the sprayed films. For the partially charged PAH at pH 9, interdiffusion is observed, as illustrated in Figure 1a, but on a much smaller scale than the dipped films. The partially charged PAH and low molecular weight PAA chains produce a film with a bilayer thickness of approximately 7.06 nm, while the longer PAA chains produce a film with a bilayer thickness of 3.72 nm. These thicknesses suggest that some interdiffusion is occurring in the smaller molecular weight PAA chain sprayed film, but not to the extent of the corresponding dipped film. Of note, the bilayer thickness of the low MW PAA dipped film is more than six times that of the sprayed film. This significant thickness difference between dip and spray LbL films at the same conditions can best be explained as the result of polyelectrolyte interdiffusion. During Spray-LbL, the polyelectrolyte solutions are forced onto the surface with a very short contact time before being rinsed away. There is less sufficient time for the polyelectrolyte chains presented at the charged multilayer surface to diffuse past the top layer before they are bombarded with the alternately charged solution from the next spray step, which rapidly forms electrostatic bonds with the underlying polyion surface layer, thus kinetically trapping them in place before they can fully diffuse into the bulk

film. It is important to note, however, that spraying does not completely inhibit the interdiffusion process. Some limited interdiffusion does occur in sprayed films, which is evident by the somewhat thicker 15k MW (7.06 nm) PAA film compared to the thinner film formed with high molecular weight PAA (3.72 nm); however, its effect is much less a factor in film growth because of the brief contact times of Spray-LbL. In films built with strong polyelectrolytes or with two fully charged weak PEs, interdiffusion does not occur¹, and Spray-LbL produces films equivalent to those of dipped LbL.^{7,8}

To further confirm that it is the short spray contact time rather than mass transport to the surface or overall surface concentration that leads to limited interdiffusion in Spray-LbL films, (PAH/PAA) films were deposited in 5 bilayer increments using higher polyelectrolyte concentrations of 20 mmol at pH=9.0 for PAH and pH=6.5 for PAA. The thickness of these films was then measured with profilometry or ellipsometry; the resulting growth curves are depicted in Figure 1 while the average bilayer thicknesses are listed in Table 6.

Table 6. Average bilayer thickness of (PAH/PAA)₂₅ using both deposition techniques at 20 mmol concentration.

Films made from 20 mmol solutions of PAH and the different PAA molecular weights. The pH value of the PAH solutions was 9.0 and the PAA solutions were at pH=6.5.

Deposition Technique	PAA Molecular Weight	PAH solution pH=9.0
Spray-LbL	15 000	14.85 +/- 0.79 nm
Spray-LbL	345 000	6.46 +/- 0.14 nm
Dip LbL	15 000	62.85 +/- 4.69 nm
Dip LbL	345 000	8.14 +/- 0.50 nm

Exponentially growing films are a clear indicator of polyelectrolyte interdiffusion in the film.¹⁹ Thus, it is expected that the 15000 molecular weight PAA films, both sprayed and dipped, should display exponential growth, while the 345000 molecular weight PAA films should exhibit more linear film

growth. Figures 24a and 24c depict the growth of the lower molecular weight PAA films deposited by spraying and dipping, respectively. Both deposition techniques clearly exhibit exponential growth with the low molecular weight PAA. This is clear evidence of the presence of interdiffusion in these two films. Figures 24b and 24d depict the growth rates of the larger molecular weight PAA films. Figure 24b becomes linear after the first 10 layers and Figure 24d becomes linear after the first 5 layers. These initial regions of non-linear growth are expected in the first few layers of most layer-by-layer films due to uneven charge distribution on the substrate surface.^{29, 30} Once this initial growth phenomenon is overcome, both of the high molecular weight PAA films grow in a relatively linear fashion. This shows that interdiffusion is not prevalent in these films as in the lower molecular weight PAA films. These growth curves are further proof that the larger molecular weight PAA hinders interdiffusion. The average bilayer thickness behaves similarly to what was found previously using the 10 mmol concentrations. The dipped film using the lower molecular weight PAA is more than 4 times thicker than the sprayed film. This is due to the diffusion limiting short contact time in the Spray-LbL process discussed earlier. The 20 mmol films are thicker than the 10 mmol solutions because during the cycle time, more polyelectrolyte chains reach the film surface in the higher concentrated solutions than the lower concentrated solutions; this is an indication that at 10 mmol concentrations and the contact time used here, the adsorption process had not reached saturation.

Further investigation indicated that the amount adsorbed continues to increase gradually with solution concentration until it levels off at a maximum film thickness, beyond which further solution concentration increases no longer yield increased film monolayer thickness. 25 bilayer films were deposited on silicon wafers by both spraying and dipping techniques using the same parameters as before, and measured with profilometry and ellipsometry. For these experiments, the PAH concentration was held constant at 20 mmol and the PAA concentration was varied from 10 mmol to 100 mmol. Only the 15 000 MW PAA was used and the pH values used were 9.0 for PAH and 6.5 for

PAA. As shown previously, this polyelectrolyte system should produce dipped films with a large amount of interdiffusion, but sprayed films with significantly less interdiffusion. As expected for both deposition techniques, as concentration increased, total film thickness also increased and eventually leveled off³¹ at approximately 80 mmol PAA concentration as shown in Figure 25.

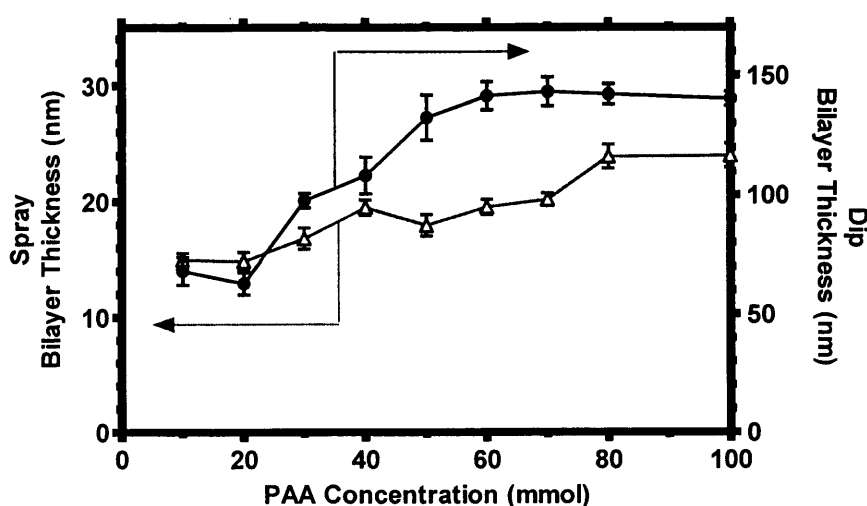


Figure 25. Correlation of Bilayer Thickness to the Number of Bilayers Both Dipped and Sprayed.

Both techniques, dip LbL (●, right axis) and Spray- LbL (Δ, left axis), produce films that increase in thickness with PAA concentration up to 80 mmol where film thickness levels off. Concentration of the PAH was held constant at 20 mmol.

The bilayer thickness for films generated from both techniques begin to level off at concentrations between 70 - 80 mmol because the films have reached their maximum surface charge density during the deposition step. This is the point of surface saturation and polyelectrolyte charge reversal, and the film thickness should not increase beyond this point with higher polyelectrolyte concentrations.³¹ There is a final equilibrium amount adsorbed beyond which further deposition is

prevented due to electrostatic repulsion at the surface, leading to a self-limiting adsorption. During this process, when interdiffusion also takes place there is absorption of chains into the LbL film as well as adsorption to the surface. This diffusion process will also be time dependent, and will increase in rate with increased solution concentration. As the solution concentration increases, the concentration gradient driving polyelectrolyte chains to the surface and/or into the film also increases. At lower PAA solution concentrations the saturation diffusion time for PAA chains in solution is greater than the dipping time, so that incomplete adsorption of PAA chains occurs during the 10 min dip. Increasing the PAA solution concentration will increase the driving force, resulting in greater adsorption of the full monolayer within the dip time frame, thus producing a thicker film. At PAA concentrations of 80 mmol or greater the saturation diffusion time of the PAA chains in solution is less than the dipping time, and the PAA chains are able to saturate the film in less than 10 min. At this point, no more polyelectrolyte can be added to the film, so any increase in polyelectrolyte concentration will not affect the film thickness.

Another way to reach the maximum charge density of the film surface is to increase the dipping time beyond 10 min. To investigate this saturation diffusion time, a 20 bilayer (PAH/PAA) film was deposited onto a SiO₂ coated QCM crystal using the automated dipping process described earlier. Once the film was deposited, it was dried over night, and then placed in the QCM-D device. An additional layer of PAH was deposited onto the crystal in the QCM-D chamber at a flow rate of 1 μ L/minute; then the crystal was rinsed in the chamber for 9 minutes with Milli-Q water. The PAA solution was introduced through the chamber and the frequency and dissipation were recorded, as shown in Figure 26. The PAA solution was allowed to flow through the chamber for over an hour. The thickness of the PAA layer formed on the top of the film leveled off entirely after 37.4min; 95% of the film mass had been adsorbed at approximately 7.5 min. The resulting dissipation fit to the Voigt model yielded a thickness for this newly deposited PAA layer of 27.3 nm. This value corresponds well to the already

discussed average bilayer thickness for a dipped film using 20 mmol concentrations of PAH and PAA of 62.8 nm (see Table 2). This result illustrates that while the 10 min contact time in dipped LbL allows sufficient time for interdiffusion, it is still too short to fully achieve polyelectrolyte equilibrium at the film surface at low solution concentrations.

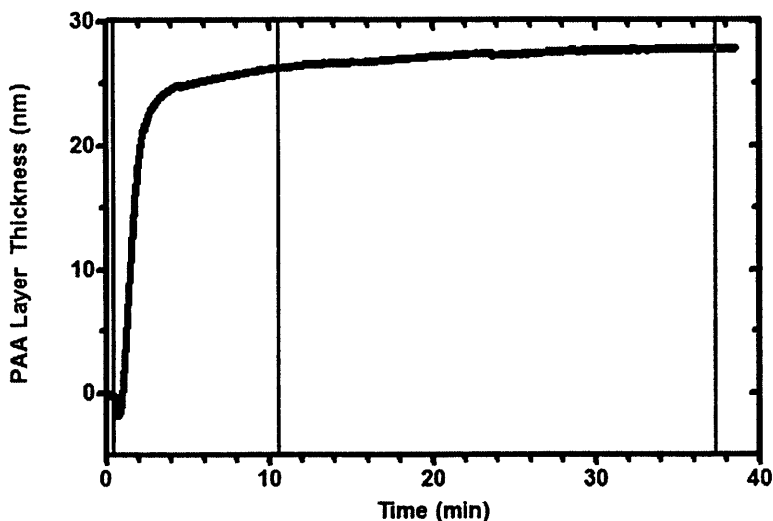


Figure 26. Growth rate of top PAA layer.

For the top PAA layer in a (PAH/PAA)₂₁ layer film. Thickness was determined by fitting the QCM-D dissipation to the Voight model using the QCM-D software. The left vertical line marks the introduction of the PAA solution to the film, corresponding to a layer thickness of 0 nm. The middle vertical line marks the elapsed time of 10 min, the normal dipping time used the dipping experiments, corresponding to a layer thickness is 26 nm. The right vertical line marks the maximum value of the PAA layer thickness, 27 nm.

As indicated by Figure 25, the Spray-LbL technique behaves in a similar manner to the dipped technique as PAA concentration is varied in that it leads to a thickness plateau at a PAA concentration of

80 mmol. However, the driving force for Spray-LbL is not just a concentration gradient between the solution and the film surface, but rather the combination of a diffusive driving force over a very short boundary layer thickness and the high-pressure, gas-driven convection introduced in the spraying process. Changing the polyelectrolyte concentration does not affect the main convective driving force, but it does affect how much polyelectrolyte comes in contact with the surface as a function of time, which enables an approach to the equilibrium thickness value during the contact period. We observe thicker films at higher concentration for this reason. Any additional polyelectrolyte chains in the sprayed water solution introduced to the surface beyond the equilibrium point will not be able to adsorb on to the surface. There is some interdiffusion occurring in the sprayed films; however, as discussed above, interdiffusion is severely limited by the short spraying contact times.

These results enable further comparisons of the Spray-LbL and Dip-LbL techniques. Both techniques produce films that increase in thickness with increasing PAA concentration up to 80 mmol, when they reach polyelectrolyte saturation and maximum film thicknesses. This finding demonstrates that both techniques build films through the alternation of electrostatic interactions, even though their driving forces and operating times are very different. Based on the interdiffusion phenomenon discussed earlier, the dipped films are much thicker than the sprayed films when there are interdiffusing species. The contact time of the spray technique of 5 s is a few orders of magnitude less than the dipping contact time of 10 min which is one third of the surface saturation diffusion time found using the QCM of 37.35 min. This simple comparison of the time scales clearly illustrates that the polyelectrolytes in sprayed films become immobilized and kinetically trapped in place, whereas the dipped films can allow for more rearrangement of the polyelectrolytes on and within the film when charge density and molecular weight of the polymer is sufficiently lowered. By increasing the concentration of the polyelectrolyte solutions or the contact time between the solutions and the film, it is possible to allow the polyelectrolytes to fully rearrange and reach equilibrium within the film.

2.4 Conclusion

In this work, we investigated the interdiffusion of PAH during deposition of (PAH/PAA)₂₅ thin films. The films were deposited using both the Dip-LbL and Spray-LbL techniques. We find that both deposition methods can exhibit some amount of interdiffusion if the polyelectrolytes are partially charged and the polyelectrolyte chains are relatively short in length. We successfully demonstrate that by using the Spray-LbL technique to deposit the thin films it is possible to severely hinder the interdiffusion of polyelectrolyte in the film compared to the dipping technique. Interdiffusion is shown to depend on three main factors: the polyelectrolyte's relative charge, the polyelectrolyte size, and the polyelectrolyte solution's contact time with the surface. By reducing the contact time through Spray-LbL, we are able to significantly reduce the interdiffusion of PAH into the film, which notably reduces the film thickness. Second, interdiffusion can be partially to fully prevented through the use of much larger polyelectrolytes in conjunction with spray-LbL. Third, using fully charged weak polyelectrolytes such as PAH at pH 6.5 severely limits interdiffusion as well. Finally, both film deposition techniques build films via the same electrostatic binding interactions, even though they work on different time scales and produce drastically different film thickness. We demonstrated that by increasing the PAA concentration that the (PAH/PAA)₂₅ films from both techniques increase in thickness until a maximum polyelectrolyte adsorption limit is reached on the film surface at a PAA concentration of 80 mmol. We also were able to demonstrate that increasing the contact time is another way to reach the maximum film thickness. These results demonstrate that faster film deposition time is not the only benefit of Spray-LbL's shorter polyelectrolyte to surface contact time compared to dipping. This shorter contact time is able to considerably hinder the interdiffusion of polyelectrolyte into the film, which can be used to control the thin film architecture of systems ranging from electrochemical to biomedical applications.

3. Film Uniformity

Abstract

The uniformity of the films produced using the automated Spray-LbL system is investigated. Films deposited on substrates greater than 1 in diameter area exhibit more than 20% variance in thickness. Adjustments were made to the setup of the system in an effort to expand the area of film thickness uniformity. However, it is determined that the design of this automated Spray-LbL system limit the film uniformity to an area of a 1 in diameter. In order to make films with a larger uniform area a different system must be developed with larger nozzles or additional nozzles arrays.

3.1 Introduction

Whether automated or hand operated, Spray-LBL has been shown to produce films of comparable quality to those of traditional Layer-by-Layer deposition^{2, 7, 17, 32}. These films are built through the sequential exposure of a substrate with a charged surface to two or more oppositely charged species. These species form electrostatic bonds with the charged surface in a self-limiting adsorption process. As previously discussed the thickness and roughness of these multilayered films is dependent on 10 main parameters of the automated Spray-LBL system. While some variation in thickness does occur across the film, it is thought to be minimal.

Izquierdo and co-workers showed that using hand operated spray cans, the largest diameter area of substrate that could be covered evenly by water droplets on paper was 5 cm.¹⁷ However, there has been no similar study to determine the largest homogenous coverage area for the automated Spray-LbL system. While conducting the optimization research in Chapter 1, the values of thickness seemed to vary by more than a few nanometers in the same film. In fact, some films had thickness variations of as

much as 100 nm between different locations on the same 25 bilayer film. These results seemed contrary to the homogenous coverage assumed for the automated system based on the work of Izquierdo et. al. Clearly the films were not as uniform as expected. This work aims to determine the area of substrate that can be uniformly coated with a variation of 20% or less in film thickness. Once this area was determined, attempts were made to increase this uniform coverage area without major modifications to the automated Spray-LbL system.

3.2 Experimental

3.2.1 Materials

Poly (acrylic acid, sodium salt) (PAA) with molecular weight of 15,000 g/mol (35% aqueous solution). Poly(ally amine hydrochloride) (PAH) molecular weight of 55 000 (powder) was purchased from Polysciences. Polymer solutions were prepared using Milli-Q water with a standard concentration of 20 mmol with respect to the repeat unit. PAH solutions were prepared at a pH of 9.0 ($pK_a \sim 8.8^{20}$) and PAA solutions were prepared at a pH of 6.5 ($pK_a \sim 6.5^{20}$). All solution pH adjustment was performed using HCl and NaOH, no additional salt was added to the polyelectrolyte or rinse solutions. Spray-LbL films were deposited on 3-inch coin roll silicon wafers (Silicon Quest International). All silicon was cleaned with ethanol and Milli-Q water to clean and hydroxylate the surface prior to deposition.

3.2.2 Deposition

(PAH/PAA)₂₅ sprayed films were constructed using the automated Spray-LbL system.⁷ All spray solutions were delivered by ultra high purity nitrogen gas (AirGas) regulated to 25psi. The PAH solution was sprayed for 4 s and allowed to drain for 5 s before spraying the rinse solution for 10 s. After 5 s for rinse drainage, the PAA solution was sprayed and rinsed similarly. This cycle was then repeated for the

desired number of bilayers, with an additional 6 s pause between bilayers. Using this setup a 25 bilayer film required approximately 20.4 min for complete deposition.

3.2.3 Analysis

Film thickness was measured using a Tencor P16 profilometer to drag a stylus across a scored film to determine the step height. A stylus tip force of 0.5 mg was used to avoid film penetration. Scratches in the film were made using a razor blade every 2 cm across the film and from top to bottom, Figure 27a. Then a thickness measurement was taken at each vertical section for a total of 42 measurements. Thickness measurements were also taken using a Woolam XLS-100 spectroscopic ellipsometer. Thickness measurements were taken in 9 places across the film, Figure 27b, to determine the thickness variation of the film. Films were dried in a nitrogen stream prior to measurement to remove any dust or other particles from the film surface.

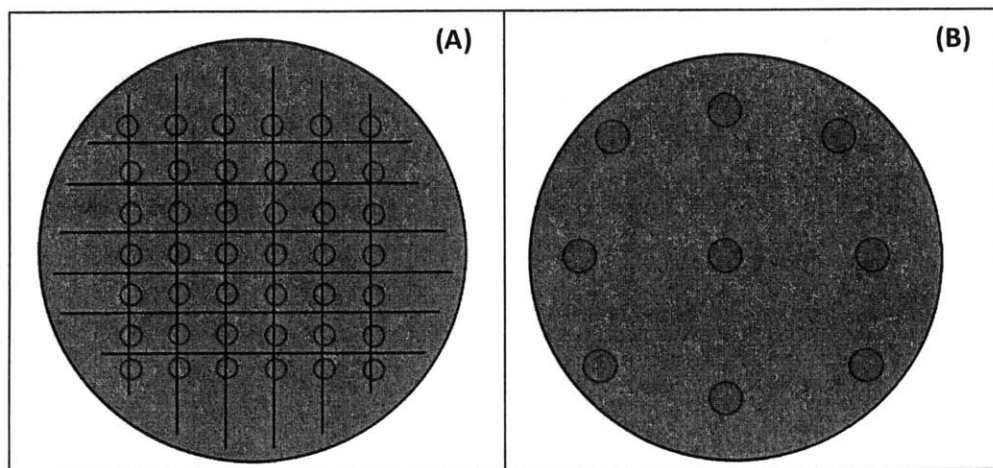


Figure 27. Locations of thickness measurements taken for film uniformity.

The red circles denote locations where film thickness was determined using either (A) the profilometer or (B) the ellipsometer.

3.3 Results and Discussion

During deposition of the films, it is possible to visibly see the film after 8 bilayers, when the refractive index of the film and reflection off of the Si wafer substrate causes a blue tint to the film. At around 12 layers, Newton rings begin to form in the film, making it obvious where the center of the film is located. Newton rings are a phenomenon related to differences in the refractive index of the film as the light travels through the film and reflects off of the silicon wafer substrate. These differences in refractive index that produce the Newton rings are due to differences in film thickness. As the film thickness changes, the resulting change in refractive index in the film produces Newton rings. At 25 bilayers, there are many Newton rings visible in the film. The presence of multiple Newton rings suggest that the film is not flat, but is thickest at the center of the Newton ring pattern and decreases as you move radially outward. While the Newton rings do indicate a thickness variation in the film, the extent of the variation was thought to be less than 20%.

By constructing a standard, Table 1, (PAH/PAA)₂₅ film and measuring the thickness at 42 different locations on the film, Figure 27a, it was possible to determine the extent of the thickness variation. Figure 28 shows the three dimensional shape of a (PAH/PAA)₂₅ film. The film thickness actually varies by approximately 223 nm or 47% from the center to the edges of the film. The automated Spray-LbL (PAH/PAA)₂₅ system does not produce flat, rectangular shaped films, it actually produces films with a dome-like shape. The uniform diameter of this film is approximately 2.5 cm or 1 inch. Beyond 1 cm from the center of the film the film thickness varies by more than 20%. These sprayed films undoubtedly have a significant thickness variation over the full radius of the Si wafer substrate. This thickness variation explains the large distribution of thickness values seen in some of the films made during the work for Chapter 1. It also better explains the visible Newton rings seen in the films deposited on Si wafers. This significant film thickness variation within the film is undesirable.

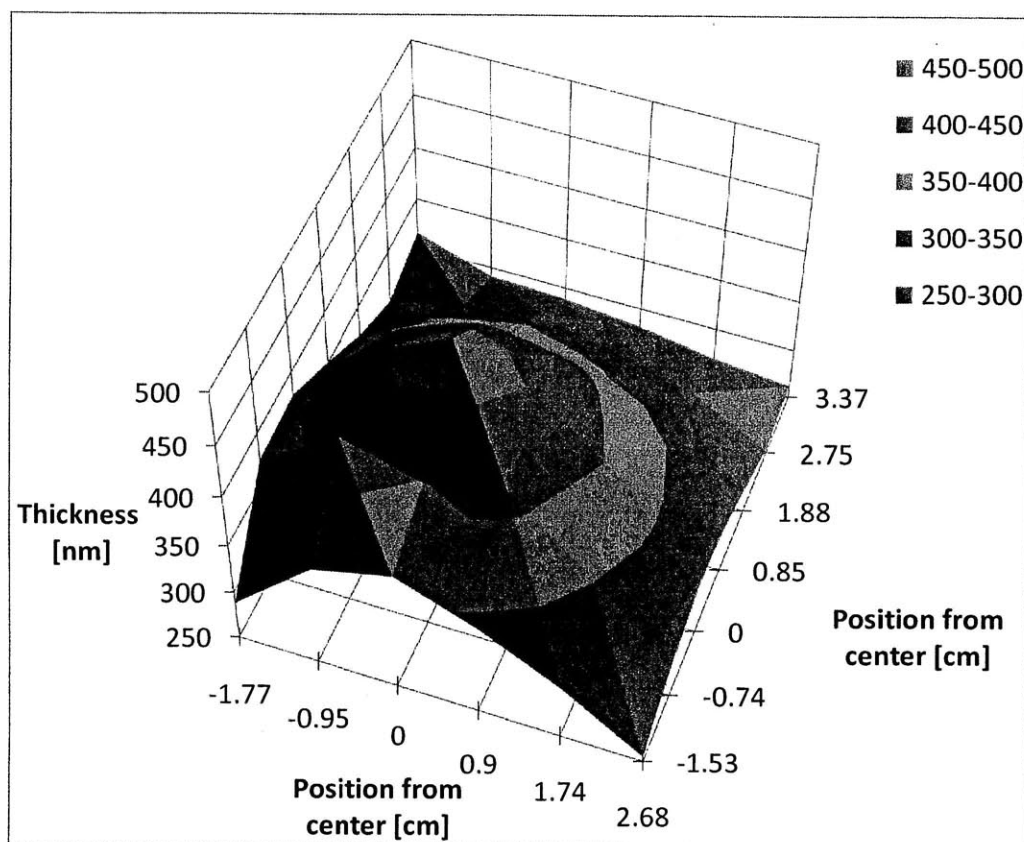


Figure 28. 3-D plot of film thickness of a standard (PAH/PAA)₂₅ film.

The 42 measurements required to produce Figure 28, required over 2 hours using the profilometer. In an effort to reduce the measurement time, the ellipsometer was used instead of the profilometer. Since the aim of this work is to reduce the film thickness variation, the main goal is to reduce the thickness difference between the center and the edges of the film. As such, the number of measurements per film was reduced from 42 to 9, Figure 27b. 8 measurements were taken at the edges of the film, and one measurement was taken at the center of the film. The 9 measurement 3-D shape of the standard (PAH/PAA)₂₅ film is shown in Figure 29. Figure 29 shows the film's shape looking parallel to

the substrate surface, as opposed to the 40° angled viewpoint of Figure 28. This parallel view allows for easier identification of the film thickness variation. The ellipsometer yields a film thickness difference of 202 nm from the center to the edge. This again is nearly 50% variation in thickness, and unacceptable.

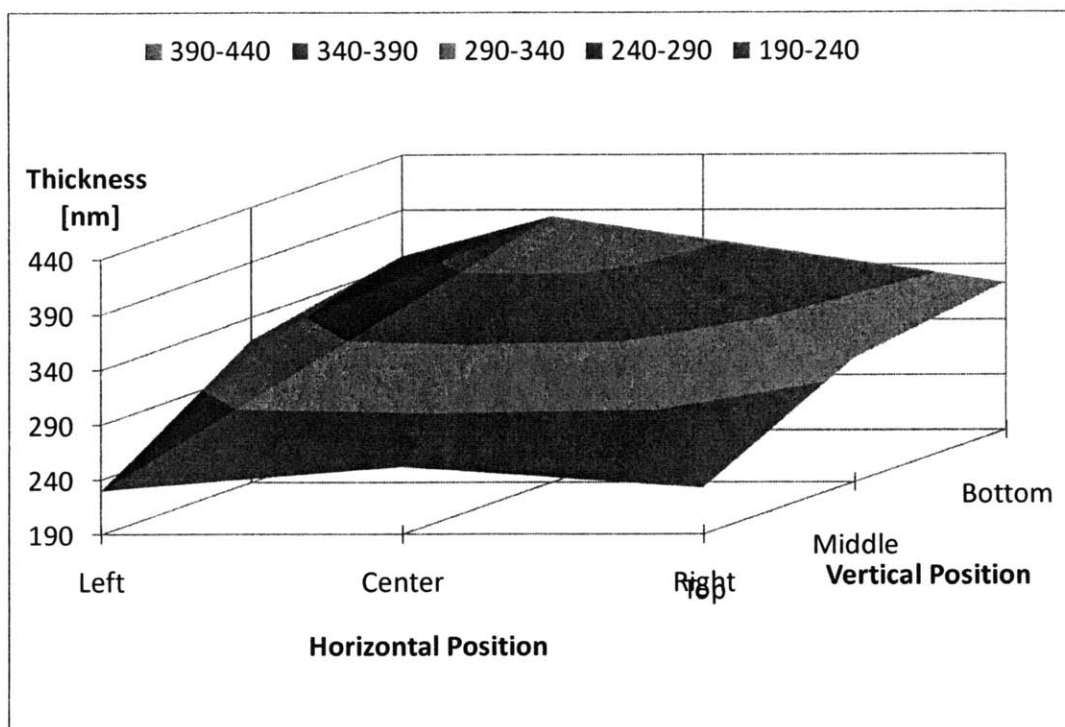


Figure 29. Parallel 3-D view of the film thickness of a standard (PAH/PAA)₂₅ film.

The significant film thickness variation poses a problem if uniform films larger than one inch in diameter are necessary. In an effort to extend the uniformity diameter of the films produced by the automated Spray-LbL system, some attempts were made at adjusting the system setup. Spraying distance was increased, and the nozzle aim points were adjusted twice.

First, the spraying distance was increased. The films produced at greater distances during the parameter optimization research seemed to have fewer visible Newton rings than the standard setup.

The 10 in spraying distance was selected because it was the smoothest film produced when adjusting the spray distance, Figure 9. Figure 30 is the 9 location thickness plot for 10 in spraying distance. The maximum thickness difference from the center to the edge for this film is approximately 184 nm. The change in film thickness seemed to be more gradual in this setup; however, the film thickness variation is over 58%. The uniform coverage area is slightly larger than the standard sample, but this setup still does not allow for uniform coverage of the 3 in silicon wafer substrate.

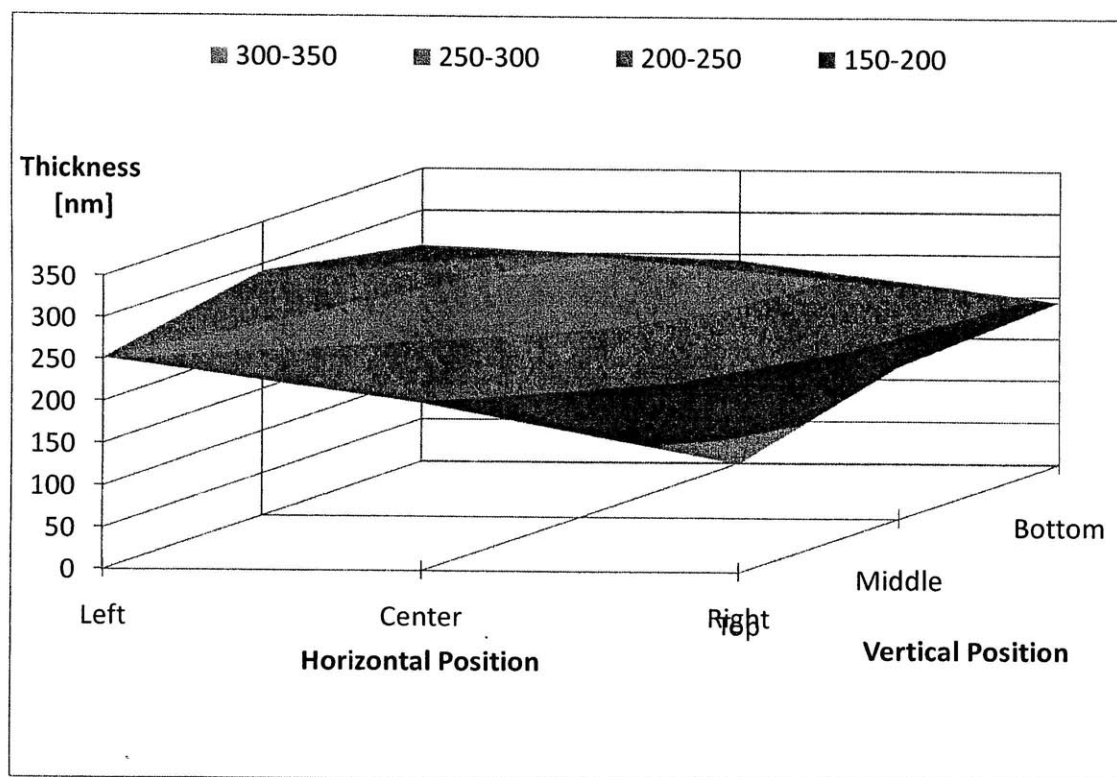


Figure 30. Parallel 3-D view of the film thickness of a (PAH/PAA)₂₅ film with spraying distance of 10 inches.

Second, the aim points of the two polyelectrolyte airbrushes were shifted to opposite sides of the substrate. The spray distance was returned to the original 7.5 inches the automated Spray-LbL is

designed for. Using my US Army artillery training for attacking a large enemy force, it was hypothesized that instead of centering the cone-shaped spray patterns on top of each other in the center of the film, that off-setting the spray patterns would extend the uniformity diameter of the film. Figure 31b illustrated the locations of the aim points and spray pattern overlap used.

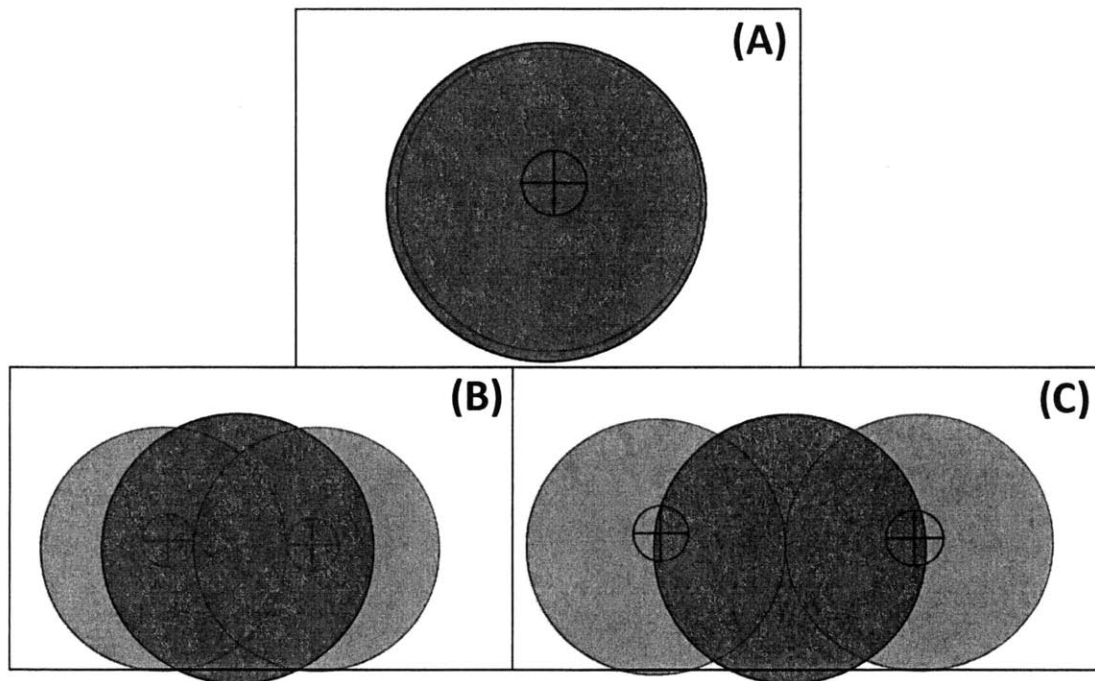


Figure 31. Aim points used to examine film uniformity.

(A) shows the centered aim points used for the films in Figures 28-30. (B) shows the offset aim points for the film in Figure 32. (C) shows the opposite edge aim points used for the film in Figure 33.

The resulting film was expected to have more of an oval-shaped thickness variation due to the overlap of the spray patterns. However, the film still had a circular-shaped thickness variation pattern. The Newton rings on this film looked nearly identical to the ones on the standard film. The maximum

film thickness of this film is less than that of the standard film, which is the main difference of these two films. Figure 32 shows the thickness variation of the film constructed using the off-set aim points. The maximum difference for this film from the center to the edge is approximately 227 nm, with a resulting thickness variation of nearly 63%. Using offset spray aim points is not a valid solution to the variation in film thickness.

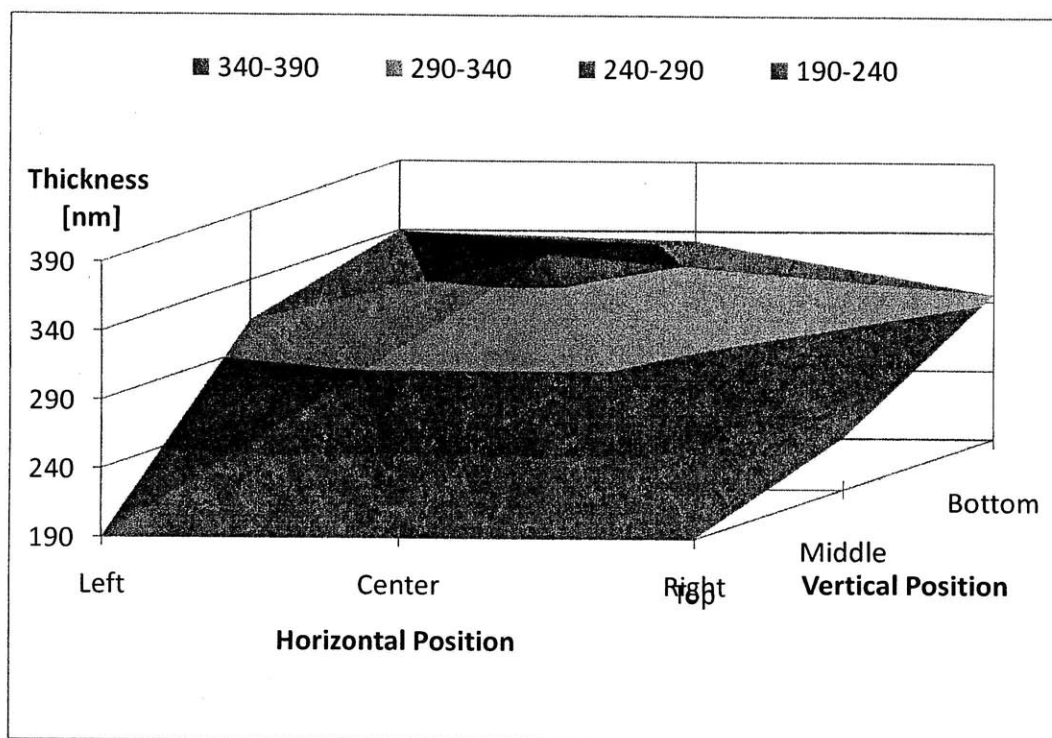


Figure 32. Parallel 3-D view of the film thickness of a (PAH/PAA)₂₅ film with offset aim points.

In one final attempt at adjusting the automated Spray-LbL system setup to reduce the film thickness variation, the aim points of the two polyelectrolyte airbrushes were adjusted to lie on either edge of the substrate. The polyelectrolyte airbrush aim points are depicted in Figure 31c. By further extending the distance between the aim points to where the spray patterns barely overlap, some difference in the film thickness variation pattern is observed. The Newton rings on this film seemed were actually

elongated oval-shaped that ran from top to bottom of the film. The maximum difference for this film from the center to the edge is approximately 184 nm, the least difference of the films examined. However, the thickness variation was the largest of any of the films, at 74%. This film was also the thinnest film produced, due to the minimal overlap of the polyelectrolyte sprays. Using offset aim points is clearly not a valid solution for increasing film uniformity.

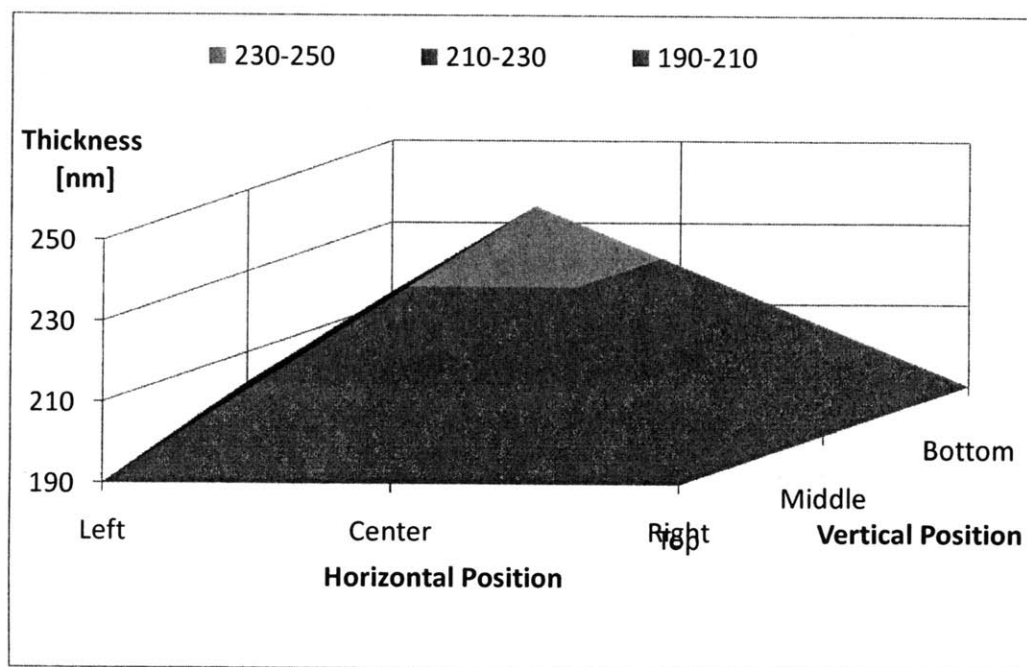


Figure 33. Parallel 3-D view of the film thickness of a (PAH/PAA)₂₅ film with aim points at the edges of the substrate.

The best way to extend the uniformity diameter for films deposited using Spray-LbL would be to use larger spray nozzles, or use just use more nozzles. However, the automated Spray-LbL system uses the largest air brushes nozzles, and is designed for a maximum of 4 air brushes. Thus, making these proposed changes is not possible with the current automated Spray-LbL system. A new system would need to be designed in order to extend the uniformity diameter of sprayed films. Svaya

Nanotechnologies, Inc. has developed automated Spray-LbL systems with more nozzles in order to deposit films on much larger substrates. Their medium sized system is able to much more uniformly coat substrates larger than 1 foot by 1 foot. Svaya provided data of a (PADC/ SiO₂ nanoparticles)₂₅ film deposited on a 16 in by 20 in pane of glass. They used a Filmetrics F-10 UV-Vis hand-held probe to measure the percent reflectance at 10 locations on this film. The resulting plot of percent reflectance versus wavelength is shown in Figure 34. This percent reflectance was then optically fit to determine the film thickness at each of the 10 measured locations. The resulting fit determined that the thickest point on the film was 175.9 nm and the thinnest point was 168.5 nm, or a thickness variation of approximately 4%. This is a significant improvement over what is possible using the smaller automated Spray-LbL system. This proves that the Spray-LbL process is scalable; however, the automated Spray-LbL system is not.

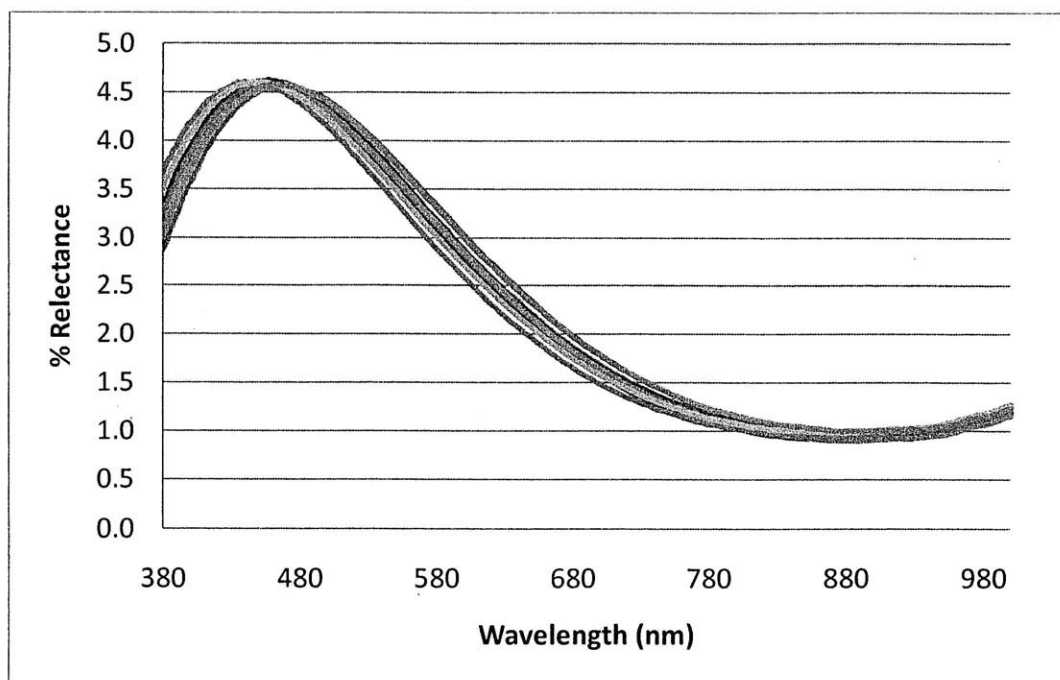


Figure 34. Percent Reflectance data for a ((PADC/ SiO₂)₂₅) film deposited using a larger Spray-LbL system. Data provided by Svaya Nanotechnologies, Inc.

3.4 Conclusion

The automated Spray-LbL system used in this work is very effective at depositing thin multilayered films on charged substrates. However, the uniformity of these films severely degrades as the distance from the center of the film increases. The films deposited using this system are fairly uniform to a diameter of around 1 inch. Beyond 1 inch in diameter, the film thickness changes by more than 15%. Thus when comparing different films, it is imperative that the thickness measurements be taken in the same relative location on each film to be compared. The thickness variation in each individual film can lead to errors in large errors when comparing different films, if the thickness measurements are not taken in the same locations. For most academic research, a 1 inch diameter is an acceptable area of uniform coverage. However, if this Spray-LbL process is to be scaled up, a new spray system, such as those developed by Svaya Nanotechnologies, Inc., must be used to adequately and uniformly deposit films.

Conclusion and Future Recommendations

The automated Spray-LbL system is a very effective technique for depositing thin, multilayered films onto substrates with a surface charge. This automated technique provides more parameters for adjusting the deposition process and thus more control in fine-tuning the deposited thin films. By analyzing the effects on film thickness and roughness of each of the 10 operational parameters of the system, it was determined that polyelectrolyte concentration, polyelectrolyte spraying time, spray distance, air pressure, and polyelectrolyte charge density are the optimal parameters for adjusting the film thickness. If evident, trends were presented for each of the 10 system parameters and their effect on film thickness. The parameter values that produced the smoothest films were also identified. These results allow for prediction and adjustment of the film properties based on the system parameter

settings, prior to spraying any solutions. This can potentially eliminate the trial and error adjustment process that is currently conducted when film thickness and/or roughness must be modified. Ideally, a similar study would be conducted using a combination of strong polyelectrolytes, such as PDAC and SPS, to determine the thickness and roughness trends for strong polyelectrolytes. The trends should be the same between the two types of polyelectrolytes, while the specific values of thickness and roughness will change. By showing the correlation between the trends of the two types of polyelectrolytes, the applications of these trends can be extended to other polyelectrolyte species.

This work also identified polyelectrolyte interdiffusion in these (PAH/PAA)₂₅ films. This interdiffusion is shown to be a function of polyelectrolyte chain molecular weight, polyelectrolyte chain charge density, and the contact time between the polyelectrolyte solution and the surface. Larger molecular weight PAA chains hindered the interdiffusion of the PAH chains, as did increasing the charge density on the PAH chains. Both of these factors have been previously proven using the traditional dipping LbL technique. However, the order of magnitude reduction in contact time from traditional LbL to Spray-LbL is shown to also severely limit the interdiffusion of PAH in the film. The very short spray times utilized in the automated Spray-LbL system, result in the polyelectrolytes that are adsorbed to the film surface to be kinetically trapped on the surface by the rapid exposure of the counter polyelectrolyte hindering the diffusion into the bulk film.

Finally, this work showed that the current automated Spray-LbL system is best used to deposit thin films not larger than a 1 in diameter area. The sprayed films are not flat or rectangular-shaped films, but rather dome-shaped films with film thickness decreasing as you move radially outward. To combat this non-uniform film thickness, several attempts were made to modify the automated Spray-LbL system; however, this uniformity diameter of 1 in seems to be dependent on the spray nozzles used in the system. The current automated Spray-LbL system in use at MIT is limited to this 1 in diameter

uniformity area due to its design. Using larger or additional nozzles should allow for the expansion of this uniform coverage area, which is shown by results from a larger scale automated Spray-LbL system developed by Svaya Nanotechnologies, Inc. If future work requires that the films be scaled up to a size larger than a 1 in diameter, then a different system must be used or developed.

References

1. Decher, G., Fuzzy nanoassemblies: Toward layered polymeric multicomposites. *Science* 1997, 277, (5330), 1232-1237.
2. Schlenoff, J. B.; Dubas, S. T.; Farhat, T., Sprayed polyelectrolyte multilayers. *Langmuir* 2000, 16, (26), 9968-9969.
3. Shiratori, S. S.; Rubner, M. F., pH-dependent thickness behavior of sequentially adsorbed layers of weak polyelectrolytes. *Macromolecules* 2000, 33, (11), 4213-4219.
4. Lee, L.; Cavalieri, F.; Johnston, A. P. R.; Caruso, F., Influence of Salt Concentration on the Assembly of DNA Multilayer Films. *Langmuir* 2006, 22, (5), 3415-3422.
5. Hu, Y.; Cai, K. Y.; Luo, Z.; Hu, R., Construction of Polyethyleneimine-beta-cyclodextrin/pDNA Multilayer Structure for Improved In Situ Gene Transfection. *Adv. Eng. Mater.* 12, (1-2), B18-B25.
6. Mamedov, A. A.; Kotov, N. A.; Prato, M.; Guldi, D. M.; Wicksted, J. P.; Hirsch, A., Molecular design of strong single-wall carbon nanotube/polyelectrolyte multilayer composites. *Nat. Mater.* 2002, 1, (3), 190-194.
7. Krogman, K. C.; Zacharia, N. S.; Schroeder, S.; Hammond, P. T., Automated process for improved uniformity and versatility of layer-by-layer deposition. *Langmuir* 2007, 23, (6), 3137-3141.
8. Krogman, K. C.; Zacharia, N. S.; Grillo, D. M.; Hammond, P. T., Photocatalytic layer-by-layer coatings for degradation of acutely toxic agents. *Chem. Mat.* 2008, 20, (5), 1924-1930.
9. Lee, D.; Rubner, M. F.; Cohen, R. E., Formation of nanoparticle-loaded microcapsules based on hydrogen-bonded multilayers. *Chem. Mat.* 2005, 17, (5), 1099-1105.
10. Park, C.; Rhue, M.; Im, M.; Kim, C., Hydrogen-bonding induced alternating thin films of dendrimer and block copolymer micelle. *Macromol. Res.* 2007, 15, (7), 688-692.
11. Kim, B. S.; Park, S. W.; Hammond, P. T., Hydrogen-bonding layer-by-layer assembled biodegradable polymeric micelles as drug delivery vehicles from surfaces. *ACS Nano* 2008, 2, (2), 386-392.
12. Zhuk, A.; Pavlukhina, S.; Sukhishvili, S. A., Hydrogen-Bonded Layer-by-Layer Temperature-Triggered Release Films. *Langmuir* 2009, 25, (24), 14025-14029.
13. Shukla, A.; Fleming, K. E.; Chuang, H. F.; Chau, T. M.; Loose, C. R.; Stephanopoulos, G. N.; Hammond, P. T., Controlling the release of peptide antimicrobial agents from surfaces. *Biomaterials* 2010, 31, (8), 2348-2357.
14. Zhang, L. B.; Li, Y.; Sun, J. Q.; Shen, J. C., Layer-by-layer fabrication of broad-band superhydrophobic antireflection coatings in near-infrared region. *J. Colloid Interface Sci.* 2008, 319, (1), 302-308.
15. DeLongchamp, D. M.; Hammond, P. T., Highly ion conductive poly(ethylene oxide)-based solid polymer electrolytes from hydrogen bonding layer-by-layer assembly. *Langmuir* 2004, 20, (13), 5403-5411.
16. Hammond, P. T., Form and function in multilayer assembly: New applications at the nanoscale. *Adv. Mater.* 2004, 16, (15), 1271-1293.
17. Izquierdo, A.; Ono, S. S.; Voegel, J. C.; Schaaf, P.; Decher, G., Dipping versus spraying: Exploring the deposition conditions for speeding up layer-by-layer assembly. *Langmuir* 2005, 21, (16), 7558-7567.
18. Felix, O.; Zheng, Z. Q.; Cousin, F.; Decher, G., Are sprayed LbL-films stratified? A first assessment of the nanostructure of spray-assembled multilayers by neutron reflectometry. *C. R. Chim.* 2009, 12, (1-2), 225-234.

19. Porcel, C.; Lavalle, P.; Decher, G.; Senger, B.; Voegel, J. C.; Schaaf, P., Influence of the polyelectrolyte molecular weight on exponentially growing multilayer films in the linear regime. *Langmuir* 2007, 23, (4), 1898-1904.
20. Choi, J.; Rubner, M. F., Influence of the degree of ionization on weak polyelectrolyte multilayer assembly. *Macromolecules* 2005, 38, (1), 116-124.
21. Szarpak, A.; Pignot-Paintrand, I.; Nicolas, C.; Picart, C.; Auzely-Velty, R., Multilayer assembly of hyaluronic acid/poly(allylamine): Control of the buildup for the production of hollow capsules. *Langmuir* 2008, 24, (17), 9767-9774.
22. Liu, H. F.; Gong, X.; Li, W. F.; Wang, F. C.; Yu, Z. H., Prediction of droplet size distribution in sprays of prefilming air-blast atomizers. *Chem. Eng. Sci.* 2006, 61, (6), 1741-1747.
23. Kirwan, L. J.; Papastavrou, G.; Borkovec, M.; Behrens, S. H., Imaging the coil-to-globule conformational transition of a weak polyelectrolyte by tuning the polyelectrolyte charge density. *Nano Lett.* 2004, 4, (1), 149-152.
24. Zacharia, N. S.; DeLongchamp, D. M.; Modestino, M.; Hammond, P. T., Controlling diffusion and exchange in layer-by-layer assemblies. *Macromolecules* 2007, 40, (5), 1598-1603.
25. Zacharia, N. S.; Modestino, M.; Hammond, P. T., Factors influencing the interdiffusion of weak polycations in multilayers. *Macromolecules* 2007, 40, (26), 9523-9528.
26. Yoo, P. J.; Zacharia, N. S.; Doh, J.; Nam, K. T.; Belcher, A. M.; Hammond, P. T., Controlling surface mobility in interdiffusing polyelectrolyte multilayers. *ACS Nano* 2008, 2, (3), 561-571.
27. Kharlampieva, E.; Kozlovskaya, V.; Chan, J.; Ankner, J. F.; Tsukruk, V. V., Spin-Assisted Layer-by-Layer Assembly: Variation of Stratification as Studied with Neutron Reflectivity. *Langmuir* 2009, 25, (24), 14017-14024.
28. Sun, B.; Jewell, C. M.; Fredin, N. J.; Lynn, D. M., Assembly of multilayered films using well-defined, end-labeled poly(acrylic acid): Influence of molecular weight on exponential growth in a synthetic weak polyelectrolyte system. *Langmuir* 2007, 23, (16), 8452-8459.
29. Ladam, G.; Schaad, P.; Voegel, J. C.; Schaaf, P.; Decher, G.; Cuisinier, F., In situ determination of the structural properties of initially deposited polyelectrolyte multilayers. *Langmuir* 2000, 16, (3), 1249-1255.
30. Park, S. Y.; Rubner, M. F.; Mayes, A. M., Free energy model for layer-by-layer processing of polyelectrolyte multilayer films. *Langmuir* 2002, 18, (24), 9600-9604.
31. Borkovec, M.; Papastavrou, G., Interactions between solid surfaces with adsorbed polyelectrolytes of opposite charge. *Curr. Opin. Colloid Interface Sci.* 2008, 13, (6), 429-437.
32. Kolasinska, M.; Krastev, R.; Gutberlet, T.; Warszynski, P., Layer-by-Layer Deposition of Polyelectrolytes. Dipping versus Spraying. *Langmuir* 2009, 25, (2), 1224-1232.

Appendix. Data tables

Difference & Prediction	Profilometer				Elipsometer		
	AVG	90% CI	Bilayer	RMS	Total	+/-	Bilayer
	Thickness		Thickness		Thickness		Thickness
	[nm]		[nm]	[Å]	[nm]	[nm]	[nm]
standard	371.2418	19.6673	14.849673	69.25	364.22	0.3757	14.5688
MW=1,200	375.2891	23.2016	15.011564	55.325	367.33	0.25593	14.6932
MW=200,000	161.4	3.41365	6.456	28.8	166.78	0.03578	6.6712
MW=1 million	256.8767	45.3307	10.275067	5140	205.55	3.272	8.222
10 mM	374.486	15.1155	14.97944	74.925	325.8	0.347	13.032
30 mM	420.317	22.8477	16.81268	61.325	441.36	0.3487	17.6544
40mM	487.445	16.1824	19.4978	83.975	472.39	0.36393	18.8956
50mM	448.9718	22.8777	17.958873	59.4	458.33	0.2813	18.3332
60mM	488.6038	16.2436	19.54415	151.575	471.53	0.59613	18.8612
70mM	504.6525	14.1513	20.1861	121.175	525.7	0.50253	21.028
80mM	598.175	25.8835	23.927	145.525	534.34	0.74622	21.3736
100mM	600.1225	25.5737	24.0049	104.85	507.58	1.5044	20.3032
150mM	566.935	17.2631	22.6774	247.075	502.04	0.72183	20.0816
200mM	544.68	25.0283	21.7872	298.625	441.25	1.6665	17.65
10psi Anion	369.119	63.5786	14.76476	97.75	414.61	0.2455	16.5844
15psi Anion	500.9667	133.886	20.038667	133.1	400.95	0.2539	16.038
20psi Anion	422.21	24.8668	16.8884	88.7	425.21	0.3091	17.0084
30psi Anion	528.62	11.5495	21.1448	66.8	458.12	0.44154	18.3248
35psi Anion	464.455	47.6575	18.5782	34.7	414.12	0.25774	16.5648
pH=6.0	515.1	7.88573	20.604	57.8	456.25	0.2669	18.25
pH=7.0	402.085	33.8517	16.0834	59.1	317.52	0.30782	12.7008
pH=8.0	179.6733	66.2737	7.1869333	57.6	226.6	0.49376	9.064
5% ETOH	425.23	43.2901	17.0092	64.6	430.68	0.23702	17.2272
10% ETOH	435.3675	23.0116	17.4147	127.05	440.24	0.3436	17.6096
20% ETOH	467.6238	13.4074	18.70495	138.6	465.14	0.51791	18.6056
30% ETOH	439.67	12.0544	17.5868	87	434.92	0.48685	17.3968
40% ETOH	400.8838	11.8744	16.03535	50.425	388.91	0.31438	15.5564
50% ETOH	340.2638	15.7227	13.61055	36.25	319.01	0.55543	12.7604
5% THF	418.25	15.8412	16.73	42.8	435.56	0.31853	17.4224
10%THF	444.635	6.78661	17.7854	95.7	439.54	0.25766	17.5816
20% THF	No Sample (Polymer immiscible in solution)						

Difference & Prediction	Profilometer				Elipsometer		
	AVG	90% C I	Bilayer	RMS	Total	+/-	Bilayer
	Thickness		Thickness		Thickness		Thickness
	[nm]		[nm]	[Å]	[nm]	[nm]	[nm]
distance 5"	522.53	29.55	20.9	125.53	531.93	0.97	21.3
distance 6"	440.00	29.58	17.6	91.75	432.47	0.66	17.3
distance 6.5"	450.45	21.97	18.0	131.38	466.30	0.79	18.7
distance 7"	379.69	18.32	15.2	120.05	393.76	0.44	15.8
8.5 " away	367.08	27.95	14.7	63.60	387.29	0.28	15.5
9.0" away	313.15	16.98	12.5	90.70	324.94	0.33	13.0
10.0" away	294.10	10.62	11.8	36.70	301.71	0.27	12.1
distance 11"	254.70	8.22	10.2	69.78	256.21	0.26	10.2
distance 12"	250.58	7.08	10.0	143.18	240.19	0.93	9.6
distance 13"	211.39	9.91	8.5	136.55	212.25	0.42	8.5
2 anion turns	318.92	24.72	12.8	80.90	326.99	0.23	13.1
3 anion turns	380.48	83.68	15.2	44.30	345.62	0.75	13.8
4 anion turns	321.03	35.70	12.8	42.60	343.88	0.22	13.8
6 anion turns	354.04	33.42	14.2	85.00	387.82	0.21	15.5
7 anion turns	379.71	27.33	15.2	103.40	400.34	0.22	16.0
8 anion turns	No Sample (7 and 8 turns have same flow rate)						
1 sec anion	276.23	19.76	11.0	45.30	289.34	0.28	11.6
2 sec anion	296.53	17.93	11.9	77.20	333.37	0.53	13.3
5 sec anion	406.13	19.14	16.2	77.40	436.77	0.25	17.5
6 sec anion	385.75	30.63	15.4	53.10	405.05	0.26	16.2
8 sec anion	445.91	17.19	17.8	204.20	436.11	0.72	17.4
10 sec anion	475.40	15.12	19.0	228.45	457.30	1.31	18.3
15 sec anion	500.22	21.20	20.0	241.70	469.35	1.27	18.8
20 sec anion	500.33	13.50	20.0	229.13	456.26	1.64	18.3
15 psi rinse	407.80	42.81	16.3	80.80	428.65	0.29	17.1
20 psi rinse	392.82	58.31	15.7	88.30	413.95	0.48	16.6
30 psi rinse	398.53	21.92	15.9	169.50	394.81	0.76	15.8
35 psi rinse	401.07	38.09	16.0	33.80	422.67	0.25	16.9
1 sec rinse	357.38	33.99	14.3	73.80	371.44	0.22	14.9
2 sec rinse	386.42	25.26	15.5	71.20	390.32	0.21	15.6
5 sec rinse	378.94	9.90	15.2	72.50	392.74	0.22	15.7
15 sec rinse	364.32	30.69	14.6	31.40	329.41	2.00	13.2
20 sec rinse	366.56	29.80	14.7	81.80	320.71	1.94	12.8
10 bilayers	32.02	17.52	3.2	29.50	49.21	0.03	4.9
20 bilayers	249.98	17.09	12.5	41.00	263.36	0.26	13.2
30 bilayers	473.50	18.58	15.8	59.00	491.24	0.30	16.4
40 bilayers	911.55	37.90	22.8	115.23	869.76	1.51	21.7
50 bilayers	979.21	36.75	19.6	107.37	715.78	7.18	14.3
60 bilayers	1561.75	41.31	26.0	179.00	1436.20	3.74	23.9
80 bilayers	2246.75	68.77	28.1	135.58	2243.60	54.10	28.0
100 bilayers	2903.00	104.56	29.0	151.68	2894.60	0.99	28.9

Difference & Prediction	Profilometer				Elipsometer		
	AVG	90% C I	Bilayer	RMS	Total	=/-	Bilayer
	Thickness		Thickness		Thickness		Thickness
	[nm]		[nm]	[Å]	[nm]		[nm]
All Press- 10 psi	333.80	9.71	13.4	90.28	327.46	0.28	13.1
All Press- 15 psi	398.91	15.39	16.0	96.90	403.85	0.45	16.2
All Press- 20 psi	447.27	20.71	17.9	108.63	448.12	0.55	17.9
All Press- 30 psi	462.55	15.55	18.5	143.58	461.61	0.70	18.5
All Press- 35 psi	552.65	18.60	22.1	220.08	504.41	1.66	20.2
PAH-10psi	311.15	18.27	12.4	239.35	-	-	-
PAH-15psi	418.03	24.70	16.7	212.45	-	-	-
PAH-20psi	404.95	28.76	16.2	171.30	-	-	-
PAH-30psi	484.97	33.30	19.4	169.93	-	-	-
PAH-35psi	478.94	22.42	19.2	250.50	-	-	-
no box	428.44	10.82	17.1	194.00	431.32	0.65	17.3
No Rinse	804.87	29.63	32.2	303.90	-	-	-
3-D Mapping	444.52	18.38	17.8	189.18	-	-	-
Noz-Cent 7.5"	386.75		15.5	#DIV/0!	394.50	0.49	15.8
Noz-Cent 10"	294.10		11.8	36.70	301.71	0.27	12.1
Noz-Overlap	346.48		13.9	#DIV/0!	342.04	0.37	13.7
Noz-Opp edge	215.43		8.6	#DIV/0!	227.58	0.36	9.1
pH=2.5/2.5	-	-	-	-	73.30	0.03	2.9
pH=5.5/5.5	-	-	-	-	244.95	0.21	9.8
pH=9.0/9.0	-	-	-	-	234.44	0.50	9.4
pH=2.5/9.0	-	-	-	-	531.08	0.96	21.2
pH=5.5/9.0	-	-	-	-	0.00	0.00	0.0
pH=9.0/9.0	-	-	-	-	0.00	0.00	0.0
pH=6.5/2.5	-	-	-	-	34.32	1.37	1.4
pH=6.5/5.5	-	-	-	-	49.54	0.03	2.0
pH=6.5/9.0	149.62	3.02	6.0	40.20	153.86	0.02	6.2
(9/6.5)15k,10mM	176.62	12.47	7.1	150.00	566.45	11.01	22.7
(9/6.5)200k,10mM	92.98	2.88	3.7	46.60	351.87	1.41	14.1
(6.5/6.5)15k,10mM	14.36	0.89	0.6	36.80	18.39	0.03	0.7
(6.5/6.5)200k,10mM	-	-	-	-	13.24	0.10	0.5

DIPPING

Difference	Profilometer				Elipsometer		
	AVG	90% CI	Bilayer	RMS	Total	=/-	Bilayer
	Thickness		Thickness		Thickness		Thickness
	[nm]		[nm]	[Å]	[nm]		[nm]
Standard	1571.17	117.17	62.8	332.73	905.25	9.82	36.2
MW ~200,000	511.90	10.40	20.5	-	-	-	-
10mM	1701.75	144.34	68.1	-	0.00	0.00	0.0
30mM	2440.75	77.55	97.6	-	1422.50	1.58	56.9
40mM	2706.50	194.19	108.3	510.07	0.00	0.00	0.0
50mM	3311.75	233.95	132.5	-	2888.30	7.28	115.5
60mM	3536.67	147.36	141.5	-	3395.60	10.92	135.8
70mM	3581.25	149.38	143.3	-	0.00	0.00	0.0
80mM	3554.33	106.38	142.2	-	0.00	0.00	0.0
100mM	3506.75	75.91	140.3	-	0.00	0.00	0.0
15k, pH 6.5/9	1090.40	31.63	43.6	336.93	667.67	6.14	26.7
200k, pH 6.5/ 9	424.43	67.56	17.0	159.23	305.26	0.77	12.2
15k, pH 6.5/6.5	148.28	28.26	5.9	-	76.46	0.45	3.1
200k, pH 6.5/ 6.5	124.74	8.70	5.0	-	28.20	0.07	1.1
DIP pH'd rinse	2377.25	44.67	95.1	385.30	1268.90	14.85	50.8
DIP mili-Q rinse	2241.25	48.80	89.7	450.90	1276.30	28.85	51.1
SPRAY pH'd rinse	377.61	25.35	15.1	218.03	310.36	1.41	12.4
SPRAY mili-Q rinse	425.17	14.41	17.0	250.48	359.16	1.22	14.4

QCM

Difference	Profilometer				Elipsometer		
	AVG	90% CI	Bilayer	RMS	Total	=/-	Bilayer
	Thickness		Thickness		Thickness		Thickness
	[nm]		[nm]	[Å]	[nm]		[nm]
SPRAY							
15k, 5 bilayers	-	-	-	-	10.85	0.08	0.4
15k, 10 bilayers	-	-	-	-	33.71	0.02	1.3
15k, 15 bilayers	-	-	-	-	105.71	0.04	4.2
15k, 20 bilayers	-	-	-	-	196.48	0.06	7.9
345k, 5 bilayers	-	-	-	-	10.34	0.22	0.4
345k, 10 bilayers	-	-	-	-	13.52	0.06	0.5
345k, 15 bilayers	-	-	-	-	59.43	0.03	2.4
345k, 20 bilayer	-	-	-	-	102.38	0.02	4.1
DIP							
15k, 5 bilayers	36.85	4.98	1.5	#DIV/0!	-	-	-
15k, 10 bilayers	205.12	2.99	8.2	#DIV/0!	-	-	-
15k, 15 bilayers	533.95	78.18	21.4	#DIV/0!	-	-	-
15k, 20 bilayers	1132.67	70.92	45.3	#DIV/0!	-	-	-
345k, 5 bilayers	36.71	4.86	1.5	#DIV/0!	-	-	-
345k, 10 bilayers	157.96	22.11	6.3	#DIV/0!	-	-	-
345k, 15 bilayers	312.87	9.65	12.5	#DIV/0!	-	-	-
345k, 20 bilayer	415.09	6.13	16.6	#DIV/0!	-	-	-

THIS PAGE LEFT
INTENTIONALLY BLANK